

Contents lists available at ScienceDirect

Food Chemistry

journal homepage: www.elsevier.com/locate/foodchem





Incorporation of brown seaweed (*Ecklonia radiata*) polyphenol crude extracts in whey protein isolate-sodium alginate emulsion delivery systems

Xinyu Duan ^a, Cundong Xie ^a, Muthupandian Ashokkumar ^b, Frank R. Dunshea ^{a,c}, Hafiz A.R. Suleria ^{a,*}

- ^a School of Agriculture, Food and Ecosystem Sciences, Faculty of Science, The University of Melbourne, Parkville, Australia
- ^b School of Chemistry, Faculty of Science, The University of Melbourne, Parkville, Australia
- ^c Faculty of Biological Sciences, The University of Leeds, Leeds, UK

ARTICLE INFO

Keywords: Antioxidant activity Seaweed polyphenols Simulated digestion Protein-polysaccharide-polyphenol complexes

ABSTRACT

Ternary complexes composed of whey protein isolate, sodium alginate, and seaweed-derived polyphenols were developed as emulsifiers to stabilize oil-in-water emulsions. Different formulations were prepared and characterized for their physicochemical properties, including particle size and surface charge. The ternary complexes produced emulsions with improved storage and thermal stability compared to other formulations, and transmission electron microscopy confirmed well-defined morphology. During simulated gastrointestinal digestion, changes in composition and antioxidant activity were monitored, revealing that the ternary complexes effectively protected lipids and bioactive compounds. This study demonstrates that combining protein, polysaccharide, and polyphenol from natural sources can yield multifunctional emulsifiers with enhanced stability and antioxidant capacity, which offer promising applications for the delivery of lipid-soluble nutrients and functional ingredients in food systems.

1. Introduction

The development of effective, multifunctional emulsifiers is a key focus in food and pharmaceutical systems, especially for improving emulsion stability and delivering bioactive compounds. Recently, the use of ternary complexes composed of proteins, polysaccharides, and polyphenols has attracted attention due to the synergistic interactions among these components. Polysaccharides can improve protein stability against both intrinsic factors (e.g., molecular conformation) and extrinsic factors (e.g., pH, ionic strength, temperature), while proteins enhance the surface activity and interfacial adsorption of polysaccharides. The addition of polyphenols further strengthens interfacial structures through covalent or non-covalent interactions, and also provides antioxidant and functional benefits (Najari et al., 2024).

Among proteins commonly used in emulsification, whey protein isolate (WPI) is a globular protein known for forming a cohesive and viscoelastic film at the oil-water interface, which reduces interfacial tension and improves emulsion stability (Li, Geng, et al., 2022). Sodium alginate (SA), a linear anionic polysaccharide derived from brown algae, forms complexes with proteins primarily through electrostatic

interactions and hydrogen bonding, and has been shown to inhibit protein aggregation near the isoelectric point (Liu et al., 2022).

In recent years, polyphenols from marine sources, particularly brown seaweeds, have gained attention because of their high antioxidant capacity and ability to interact with proteins. However, most studies on ternary systems have concentrated on commercially available phenolics (e.g., gallic acid, tannic acid), while polyphenols from seaweeds remain less studied. *Ecklonia radiata*, one of the most abundant brown seaweeds along Australian coasts, is rich in unique phlorotannins and other phenolic compounds (Duan et al., 2024). Despite its abundance, its use in emulsion systems is still largely unexplored.

Therefore, this study aimed to develop a new ternary emulsifier system using WPI, SA, and polyphenols extracted from *E. radiata*, and to systematically assess its physicochemical properties and digestive behavior in oil-in-water emulsions. It is hypothesized that adding seaweed-derived polyphenols into the WPI-SA matrix would improve emulsion stability and antioxidant activity, especially under simulated gastrointestinal conditions. This work is innovative because it utilizes a locally underused marine bioresource and provides a thorough investigation of the interactions between protein, polysaccharide, and

E-mail address: hafiz.suleria@unimelb.edu.au (H.A.R. Suleria).

 $^{^{\}ast}$ Corresponding author.

polyphenol components, as well as their interfacial behavior during digestion.

2. Materials and methods

2.1. Materials and reagents

Fresh *E. radiata* samples were collected in February 2024 (late summer) from Queenscliff Harbor (Queenscliff, VIC, AU) using random sampling along the intertidal zone. Species identification was confirmed at Deakin University's Queenscliff Marine Science Center (Queenscliff, VIC, AU). To minimize variability, samples were harvested in bulk (>1 kg wet weight), immediately transported to the laboratory on ice, and processed within 4 h.

WPI (> 90 % protein, < 0.6 % sugar) was purchased from BIOFLEX Pty Ltd. (Grove, TAS, AU). SA (CAS No. 9005-38-3; viscosity: 5.0-40.0 cps in 1 % water at 25 °C; analytical grade) was obtained from Sigma-Aldrich Pty Ltd. (Macquarie Park, NSW, AU). Canola oil (100 % oil, < 0.1 % protein; cold-pressed, food grade) was sourced from Woolworths Group Ltd. (Melbourne, VIC, AU). Enzymes used for in vitro digestion included porcine trypsin (CAS No. 9002-07-7), pepsin (from porcine gastric mucosa, CAS No. 9001-75-6) and bile salts all sourced from Sigma-Aldrich Pty Ltd. (Macquarie Park, NSW, AU); pancreatin (from porcine pancreas, CAS No. 8049-47-6) from US Biological (Salem, MA, USA); and porcine trypsin from Southern Biological Pty Ltd. (Alphington, VIC, AU). Standard chemicals were all obtained from Sigma-Aldrich Pty Ltd. (St. Louis, MO, USA), including gallic acid (CAS No. 149-91-7), bovine serum albumin (BSA, CAS No. 9048-46-8), D-galacturonic acid (CAS No. 91510-62-2), and Trolox (CAS No. 53188-07-1). All other reagents were of analytical or HPLC grade unless otherwise specified.

2.2. Polyphenol crude extraction

The crude extract was prepared following our previous study with modifications (Duan et al., 2024). Upon arrival, fresh *E. radiata* samples were thoroughly washed with tap water, then rinsed with Milli-Q water to remove surface debris, salts, and epiphytes. The cleaned seaweed was blotted dry, cut into approximately 1–3 cm segments with a stainless-steel food-grade knife, and immediately stored at $-20~^{\circ}$ C. Before extraction, frozen samples were thawed at 4 $^{\circ}$ C and finely chopped into roughly 1 cm pieces.

For crude polyphenol extraction, 50 g of chopped seaweed was soaked in 250 mL of an ethanol-water mixture (80:20, v/v) in an amber flask and agitated at 120 rpm for 16 h at room temperature. The extract was then centrifuged at 8000g for 15 min at 4 °C using a Hettich Refrigerated Centrifuge (ROTINA380R, Tuttlingen, Baden-Württemberg, Germany). The supernatant was collected, filtered through a 0.45 μ m Millipore syringe filter (Billerica, MA, USA), and immediately freezedried using a Dynavac FD3 (Belmont, WA, Australia). The resulting powder was designated as seaweed polyphenol extract (SP) and stored at -20 °C in airtight vials until further use. The chemical profile of SP was previously characterized using LC-ESI-QTOF-MS/MS (Duan et al., 2024).

2.3. Preparation of emulsions

WPI (3 wt%), SA (2.5 wt%), and SP (2 wt%) stock solutions were freshly prepared by dissolving the respective powders in deionized water under constant stirring. The WPI-SA-SP emulsion was formulated with a canola oil-to-water phase ratio of 2:5 (w/w), where the aqueous phase comprised a 1:1:1 (w/w/w) mixture of the WPI, SA, and SP solutions. The selected concentrations were determined based on preliminary trials evaluating multiple formulations with varying levels of protein, polysaccharide, and polyphenol. Among these, the current formulation exhibited the greatest storage stability and was therefore selected for further analysis.

Control formulations were prepared by substituting one of the functional components with deionized water (W) to generate WPI-SA-W, WPI-W-SP, and WPI-W-W emulsions. Each emulsion was initially homogenized with a high-speed mixer (T25 Digital Ultra-Turrax, IKA, Staufen, Germany) at 13,500 rpm for 3 min, then further homogenized using a high-pressure homogenizer (GEA Lab Homogenizer PandaPLUS 1000, Parma, Italy). The high-pressure homogenization was carried out at 500 \pm 20 MPa for five cycles to produce fine, stable emulsions. Additionally, emulsions formulated as W-SA-SP, W-SA-W, and W-W-SP were pre-tested and found to be physically unstable; therefore, they were excluded from further analysis. A blank oil-water control (O—W) was also prepared using the same oil-to-water ratio, but without the addition of emulsifying components, to serve as a reference for assessing oil behavior in the absence of biopolymers.

2.4. Physicochemical properties of emulsions

2.4.1. Particle size and ζ-potential

Particle size and $\zeta\text{-potential}$ of the emulsions were measured using a Zetasizer Nano ZS (Malvern Instruments, Worcestershire, UK). Before analysis, samples were diluted 100 times with deionized water to reduce multiple scattering effects. The refractive index was set to 1.45, matching that of protein-based systems, and water was used as the dispersant medium for all measurements. Each measurement was performed in triplicate at 25 °C, and the results are reported as mean \pm standard deviation.

2.4.2. Morphological feature

Preliminary morphological characteristics of the emulsions were observed using an optical microscope (OM) (Leica ICC50 W, Germany). A single drop of each emulsion was placed on a clean glass slide, covered with a coverslip, and examined under $40\times/0.65$ magnification.

For nanoscale structural characterization, a transmission electron microscope (TEM) (Tecnai Spirit, FEI, USA) was employed. Emulsion samples were diluted in deionized water to a final concentration of 2 mg/mL, and 10 μL of the diluted emulsion was deposited onto a carbon-coated copper grid. After allowing the sample to adsorb, excess liquid was gently wiped off using filter paper. The grids were then dried at 25 $^{\circ}$ C, stained with phosphotungstic acid (10 mg/mL, pH \sim 7.0) for 2 min, and air-dried before imaging. TEM observations were carried out at an accelerating voltage of 100 kV.

2.4.3. Creaming index (CI)

Emulsion samples (5 mL each, in triplicate) were transferred into clean glass vials and sealed with screw caps. The vials were stored at room temperature under static conditions for stability monitoring. The creaming index (CI) was calculated as the percentage of the height of the serum layer (bottom phase) relative to the total height of the emulsion column, using the following equation:

$$CI\left(\%\right) = \frac{H_s}{H_r} \times 100\% \tag{1}$$

where H_s is the height of the serum layer, and H_T is the total height of the emulsion samples. Measurements were taken at predetermined time intervals using a digital vernier caliper to ensure accuracy.

2.4.4. Apparent viscosity

The apparent viscosity of the emulsions was measured using a twindrive rheometer (Anton Paar MCR 702, Austria) equipped with a concentric cylinder measuring system (Peltier cup: C-CC27/T200/SS). A fixed gap of 0.010 nm was maintained during all measurements. Viscosity was recorded as a function of shear rate over the range of 0.1 to $100~\text{s}^{-1}$ at three temperatures: 4 °C, 25 °C, and 37 °C.

2.4.5. Differential scanning calorimetry (DSC)

The thermal stability of the emulsions was assessed using a Nano Differential Scanning Calorimetry (DSC, TA Instruments). For each measurement, 20 μL of emulsion was loaded into a hermetically sealed aluminum sample pan, while deionized water was used in the reference cell as the baseline. The thermal program consisted of a heating-cooling loop from 10 °C to 80 °C and back to 10 °C, with a constant scan rate of 1 °C/min. Before analysis, samples were equilibrated at 10 °C for 5 min. All measurements were performed under a nitrogen atmosphere to prevent oxidative degradation.

2.5. In vitro stimulated digestion

2.5.1. Digestion procedure

The *in vitro* digestion of emulsions was conducted following the protocol based on the standardized INFOGEST 2.0 static model (Brodkorb et al., 2019). Simulated digestive fluids, including simulated salivary fluids (SSF), gastric fluid (SGF), and intestinal fluid (SIF), were prepared accordingly.

Oral phase:

A 5 mL aliquot of emulsion was mixed with 5 mL of SSF containing $\alpha\text{-amylase}$ (75 U/mL) and incubated at 37 $^{\circ}\text{C}$ in a thermostatic shaker. Samples were collected after 2 min and 30 min.

Gastric phase:

The 2-min oral digestate was mixed with an equal volume of SGF and adjusted to pH 3.0 using 6 M HCl. Digestion was initiated by adding porcine pepsin to a final enzyme activity of 2000 U/mL. Samples were incubated at 37 $^{\circ}$ C, and aliquots were collected after 0, 1, 2, and 3 h.

Small Intestinal phase:

The 2-h gastric chyme was combined with an equal volume of SIF and neutralized to pH 7.0 using 1 M NaOH. The mixture was supplemented with digestive enzymes and bile salts to mimic intestinal conditions: bile salts (10 mM), bovine chymotrypsin (25 U/mL), porcine trypsin (100 U/mL), porcine pancreatic α -amylase (200 U/mL), and porcine pancreatic lipase (2000 U/mL). Samples were incubated at 37 °C, with collection after 0, 1, 2, and 3 h.

Positive control (sample mixed with deionized water), negative control (deionized water mixed with digestive fluids), and prolonged digestion control (sample mixed with digestive fluids; incubation times: oral 30 min, gastric 3 h, and intestinal 3 h) were prepared.

At each stage, a portion of the sample was immediately taken for particle size and ζ -potential analysis, while the remainder was rapidly snap-frozen in liquid nitrogen to inactivate enzymatic activity and stored for further analysis.

2.5.2. Determination of chemical composition

The total phenolic content (TPC) was determined using a modified Folin-Ciocalteu colorimetric method (Wu et al., 2022). Briefly, 25 μL of the sample was mixed with an equal volume of Folin reagent (1:3, ν/ν) and 200 μL of deionized water in a 96-well plate. After incubation at room temperature for 5 min, 25 μL of 10 % (w/ν) sodium carbonate solution was added. The mixture was further incubated at room temperature for 60 min, and its absorbance was measured at 765 nm. Gallic acid (0–1 mg/mL) was used for calibration, and the results were expressed as milligrams of gallic acid equivalents per gram of sample (mg GAE/g).

The protein content was quantified using the Bradford assay (Bradford, 1976). In short, 5 μ L of the sample was mixed with 250 μ L of Bradford reagent. After shaking for 30 min, the mixture was incubated in the dark room at room temperature for 20 min. Absorbance was then measured at 595 nm. BSA (0–0.35 mg/mL) was used as the standard.

The uronic acid content was measured using the carbazole-sulfuric acid method (Bitter & Muir, 1962). In brief, 1 mL of sample was added to a 50 mL Falcon tube, followed by 6 mL of concentrated sulfuric acid while the tube was kept in an ice bath. The mixture was thoroughly shaken and then heated at 85 °C for 20 min. After cooling to room

temperature, 0.2 mL of 0.1 % (w/v in ethanol) carbazole solution was added, and the mixture was incubated at room temperature for 2 h. Subsequently, 300 μ L of the mixture was transferred to a 96-well plate, and absorbance was measured at 530 nm. D-galacturonic acid (0.1–0.6 mg/mL) was used as the standard.

2.5.3. Estimation of antioxidant capacity

The 2,2-diphenyl-1-picrylhydrazyl (DPPH) radical scavenging capacity and hydroxyl (•OH) radical scavenging of emulsion samples were determined using the method modified by Xie et al. (2024). Trolox (0–1 mg/mL) and ascorbic acid (0–1 mg/mL) were used as standard equivalents for the DPPH and •OH assays, respectively. To improve accuracy, the absorbance of both the reagent blank (DPPH with solvent) and the sample solvent blank (sample with solvent without DPPH) was subtracted from the measured absorbance to eliminate background interference. The radical scavenging capacity was calculated using the following equation:

Scavenging capacity (%) =
$$\left(1 - \frac{A_{sample} - A_{blank}}{A_{control} - A_{blank}}\right) \times 100\%$$
 (2)

where A_{sample} is the absorbance of the sample (DPPH solution with sample), A_{blank} is the absorbance of the sample with solvent (without DPPH, corrects for sample color/impurities), $A_{control}$ is the absorbance of the DPPH solution with solvent (reagent blank).

2.5.4. Estimation of free fatty acid release (FFA)

The amount of released free fatty acids (FFAs) was calculated from the titration curve, assuming that each triacylglycerol molecule yields two FFAs upon hydrolysis. This calculation followed the principles of acid value determination for fats and oils, as described in the American Oil Chemists' Society (AOCS) Official Method Cd 3d63 (AOCS, 2017). The percentage of FFAs released was determined from the volume of potassium hydroxide (KOH) required to neutralize the FFAs, according to the following equation:

$$FFA~(\%) = \frac{V_{KOH} \times M_{KOH} \times M_{lipid}}{2\omega_{lipid}} \times 100\%$$
 (3)

where V_{KOH} is the volume of KOH used for titration (mL), M_{KOH} is the molar concentration of KOH solution (mol/L), M_{lipid} is the molecular weight of the primary fatty acid (g/mol), and ω_{lipid} is the initial mass of oil in the emulsion (g).

2.6. Statistical analysis

All experiments were performed in triplicate, and results are presented as mean \pm standard deviation (SD). Statistical significance among groups was evaluated using one-way analysis of variance (ANOVA), followed by Tukey's post hoc test to identify pairwise differences. Analyses were conducted using Minitab statistical software (version 19.2020.1.0; Minitab Inc., State College, PA, USA), with a significance level set at p < 0.05. All figures were generated using Graph-Pad Prism (version 10.0.3; GraphPad Software, San Diego, CA, USA).

3. Results and discussion

3.1. Physicochemical properties of emulsion systems

3.1.1. Particle size

The particle size and ζ -potential of the four emulsions are presented in Table 1. Previous studies reported that WPI-stabilized emulsions typically have particle sizes ranging from 370 to 750 nm (Ye et al., 2021). Our findings were within this range, with sizes significantly influenced by the presence of SA (p < 0.05). Specifically, WPI-SA-W and WPI-SA-SP emulsions exhibited significantly smaller particle sizes (377.5 \pm 3.76 nm and 428.8 \pm 5.42 nm, respectively) compared to WPI-

Table 1
Particle mean sizes, polydispersity index (PDI) values, and ζ-potential of different emulsions

Formulations	Particle sizes (nm)	PDI (-)	ζ-potential (mV)
WPI-SA-SP	428.8 ± 5.42^{c}	0.19 ± 0.004^a	$-47.2 \pm 1.07^{\rm b}$
WPI-W-SP	$472.3 \pm 2.76^{\rm b}$	0.37 ± 0.013^{b}	$-29.6\pm0.65^{\mathrm{c}}$
WPI-SA-W	$377.5 \pm 3.76^{\mathrm{d}}$	0.14 ± 0.001^{a}	-50.5 ± 0.57^{a}
WPI-W-W	634.0 ± 4.91^{a}	$0.41 \pm 0.057^{\mathrm{b}}$	-24.9 ± 0.49^{d}

WPI, whey protein isolate; SA, sodium alginate; SP, seaweed polyphenol; W, deionized water. Different lowercase letters (a-d) indicate significant differences (p < 0.05) between absolute values according to Tukey's multiple comparison test.

W-W and WPI-W-SP (472.3 \pm 2.76 and 634.0 \pm 4.91 nm, respectively). This reduction in particle size upon SA addition was attributed to the formation of compact protein-polysaccharide complexes, driven by electrostatic attraction between the negatively charged carboxyl groups in SA and the positively charged amino groups in WPI (Yadollahi et al., 2023). This mechanism was further supported by Liu et al. (2022), who observed a 65 % decrease in the particle size of WPI-SA dispersions compared to WPI alone at pH 5.0, with similar trends reported across a broad pH range. However, some contrary findings suggested that adding SA could increase particle sizes instead, with SA concentration and accompanying pH variations considered the principal reasons (Kim et al., 2022).

Our results were further supported by the polydispersity index (PDI) values, which reflect particle size distribution uniformity. WPI-SA-SP and WPI-SA-W exhibited low PDI values of 0.19 and 0.14, respectively, indicating narrow, monodisperse size distributions, consistent with more stable emulsions (Danaei et al., 2018). In contrast, WPI-W-SP and WPI-W-W showed higher PDIs of 0.37 and 0.41, which suggested more heterogeneous emulsions with broader droplet distribution. This further demonstrated the stabilizing effect of SA in limiting coalescence and aggregation during emulsification.

In terms of SP, the addition of SP yielded contrasting effects depending on the systems. Compared to WPI-SA-W, WPI-SA-SP had a slightly increased particle size, while compared to WPI-W-W, the WPI-W-SP sample showed a significantly smaller particle size (p < 0.05). This dual behavior could be due to polyphenol-induced protein-protein aggregation through hydrogen bonding and hydrophobic interactions (Chen et al., 2023), which may either promote flocculation or, conversely, enhance interfacial adsorption depending on the formulation matrix. For example, Xu et al. (2022) reported that after covalent binding with polyphenol, the average particle size of the soy proteinferulic acid emulsion decreased from 282.77 \pm 0.67 nm to 243.07 \pm 0.25 nm, which was possibly due to the enhanced emulsifying property of proteins. In contrast, Song and Yoo (2017) reported that high concentrations of tea polyphenols led to emulsion destabilization via bridging flocculation and protein dimerization. Our results suggested that in SA-free systems, polyphenols favored the formation of stable protein-polyphenol complexes that improve emulsification, whereas in SA-containing systems, competitive binding or structural interference may counterbalance this effect.

The ζ -potential across all emulsions exceeded |25~mV|, which indicated comparable colloidal stability. SA significantly enhanced the negative surface charge, with WPI-SA-SP and WPI-SA-W showing ζ -potentials of $-47.2 \pm 1.07~\text{mV}$ and $-50.5 \pm 0.57~\text{mV}$, respectively, compared to $-29.6 \pm 0.65~\text{mV}$ (WPI-W-SP) and $-24.9 \pm 0.49~\text{mV}$ (WPI-W-W) (p < 0.05). This increase was attributable to the polyanionic nature of SA and the formation of electrostatically stabilized complexes with WPI (Kim et al., 2022).

The addition of SP led to a marginally less negative surface charge in the SA-containing system, likely due to the competitive binding between SA and SP for WPI interaction sites, which may have altered the interfacial composition or partially neutralized surface charges (Soares et al.,

2009). In contrast, in the absence of SA, the incorporation of SP significantly increased the magnitude of the negative ζ -potential, which suggested SP-induced conformational changes in WPI that exposed more negatively charged residues (Yan et al., 2020). Similar observations were reported by Tang et al. (2025), who showed that polyphenols can alter protein interfacial structures through both non-covalent and covalent interactions, thereby influencing the spatial orientation and exposure of charged amino acid residues. In their study, emulsions formed using rosmarinic acid and caffeic acid with pea protein exhibited ζ -potentials of -26.06 mV and -24.59 mV, respectively, supporting the notion that polyphenols with higher hydroxyl group content can more effectively restructure proteins and enhance the exposure of internal anionic groups.

3.1.2. Storage stability

The storage stability of the emulsions was assessed based on the CI values and OM images. All freshly prepared emulsions exhibited a uniform appearance: SP-containing samples appeared light beige, while those without SP were milk white (Fig. 1b). By Day 6, WPI-W-SP exhibited clear phase separation, forming multilayer systems characterized by a cream layer (indicated by red arrows) and a serum layer (blue arrows). The distinct and clear serum layer at the bottom indicated that the majority of droplets and aggregates had migrated upward, possibly due to the influence of SP. The brownish hue of the emulsion layer further suggested the flotation of polyphenol-containing particles, which may have adsorbed onto droplet surfaces and induced bridging flocculation (Xie et al., 2023).

Although ζ -potential results indicated that SP increased surface negativity, which generally favors colloidal stability through enhanced electrostatic repulsion, the observed three-layer separation in the WPI-W-SP system suggested that other interactions, such as polyphenol-mediated bridging flocculation and potential synergistic or competitive effects between polyphenols and polysaccharides, may dominate the system's behavior and lead to phase separation. Similar results were reported for SA-stabilized emulsions, supporting the hypothesis of complex interplays between polyphenols and polysaccharides (Yan et al., 2021).

CI data (Fig. 1a) revealed that phase separation in non-SA emulsions began on Day 2, increased through Day 4, and plateaued at approximately 14.50 %. In contrast, significantly lower and more stable values (~2.90 %) were observed in SA-containing emulsions. This observation reflected a temporal hysteresis effect, defined here as a delay in the onset of visible phase separation (e.g., creaming) during storage, rather than a difference in the ultimate extent of instability. Specifically, WPI-SA-W and WPI-SA-SP began separating on Day 3 and Day 4, respectively. This delayed separation might be attributed to the viscoelastic nature of SA, which increases emulsion viscosity and thereby retards droplet migration (Kuang et al., 2023). Additionally, protein-polysaccharide conjugates may form a multilayer interfacial structure that reduces oil migration and inhibits droplet aggregation (Li, Liu, et al., 2022).

While both WPI-SA-SP and WPI-SA-W showed similar final CI values, the slightly later onset of separation in WPI-SA-SP suggested that SP may subtly exert interfacial properties. However, no clear synergistic effect on stability was observed. Instead, interactions between SA and SP with WPI likely involve complex and possibly competitive mechanisms, such as co-adsorption, spatial hindrance, or redistribution of interfacial components, which may influence the emulsification and stabilization behavior (Petrut et al., 2016). Similarly, WPI-W-SP showed a delayed onset of separation compared to WPI-W-W, supporting that SP alone may contribute to a moderate hysteresis effect via interactions with proteins and droplet surfaces (Luo et al., 2011).

OM was employed to monitor structural changes in emulsion droplets during storage (Fig. 2). Notably, all OM micrographs were captured using a consistent scale bar of 0.5 μm to facilitate qualitative comparison between formulations in terms of visible droplet growth, aggregation, and morphology.

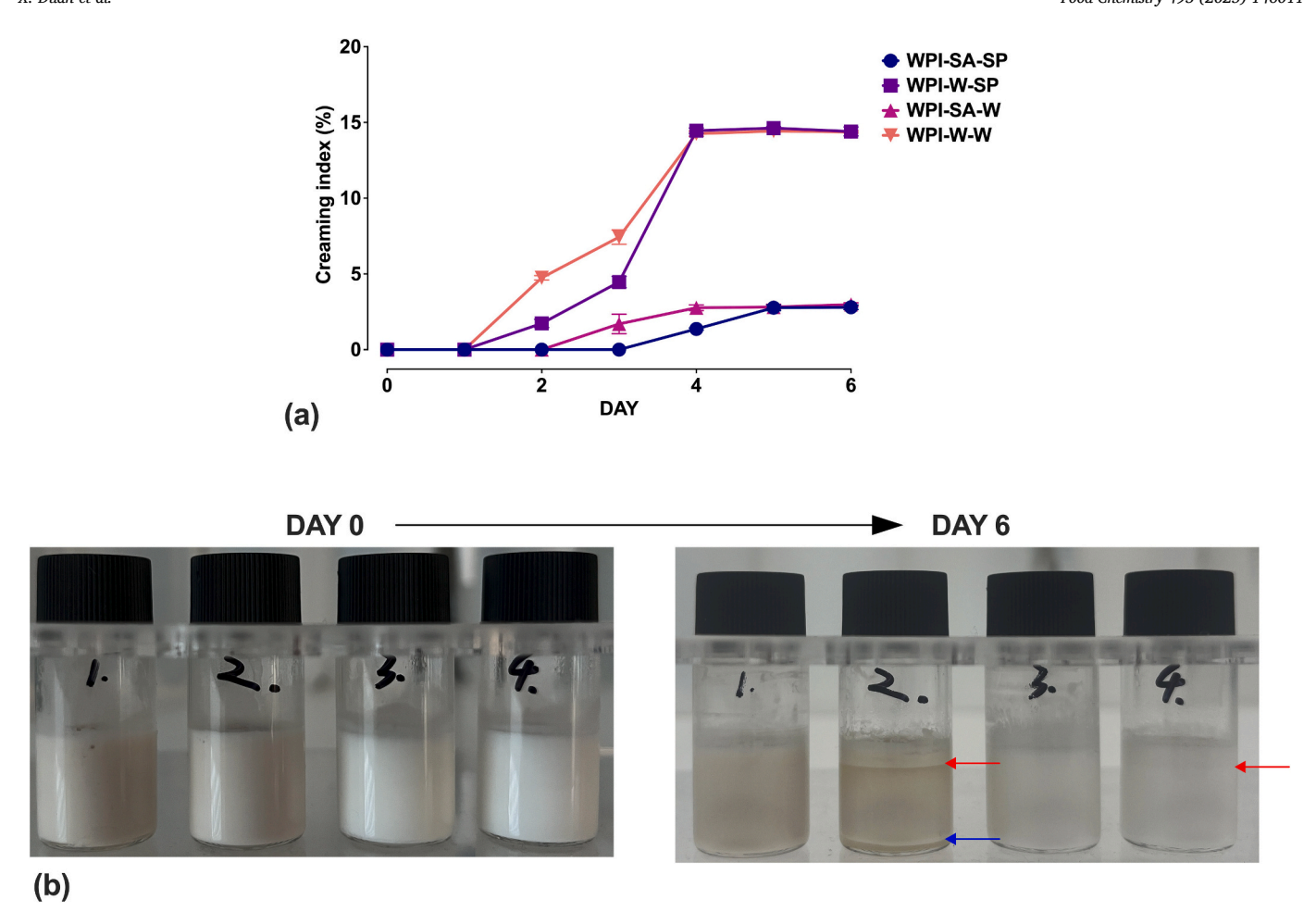


Fig. 1. Storage stability of emulsion formulations. (a) Creaming index (CI, %); (b) Storage stability at room temperature, samples 1–4 correspond to WPI-SA-SP, WPI-W-SP, WPI-SA-W and WPI-W-W, respectively. WPI, whey protein isolate; SA, sodium alginate; SP, seaweed polyphenol; W, deionized water.

Freshly prepared samples showed relatively uniform droplet sizes only in the WPI-SA-SW system, indicating optimal stabilization due to balanced interactions among protein, polysaccharide, and polyphenols. During storage, all formulations exhibited increased droplet size, possibly caused by coalescence; however, extensive aggregation did not occur in the WPI-SA-SP system. A comparable trend appeared in WPI-SA-W, although aggregation was more pronounced. The presence of SP appeared to promote cross-linking with proteins at the interface to enhance film integrity and potentially form a more compact interfacial network. In contrast, the emulsion solely stabilized by protein and polyphenols (WPI-W-SP) revealed pronounced droplet aggregation, forming grape-like clusters. Such an appearance was also reported by Bhattarai et al. (2019), who defined it as open association ("open" flocs). Insufficient emulsifying ability normally leads to a reduction in interfacial repulsive forces, such as electrostatic repulsion and steric hindrance, causing the oil droplets to undergo open flocculation more rapidly, where droplets aggregate into a network structure through weak attractive forces without coalescing.

3.1.3. Thermal stability

Changes in heat flow and apparent viscosity were used to assess the thermal stability of emulsions at different temperatures (Fig. 3). DSC analysis revealed that WPI-SA-SP and WPI-SA-W exhibited relatively stable heat flow between -2100 and $-2060~\mu\text{W}$ during the heating process, indicating higher thermal stability compared to WPI-W-SP ($\sim\!2600~\mu\text{W}$). These results suggested that the inclusion of SA played a key role in improving temperature resistance to temperature-induced physical changes, likely by forming a protective network structure

with WPI. Previous studies have demonstrated the protective effect of polysaccharides on WPI against heat-induced aggregation (Setiowati et al., 2016). The additional presence of SP in WPI-SA-SP did not markedly alter the thermal profile compared to WPI-SA-W, which showed that SP may have had a minimal or negligible effect on thermal behavior under these conditions.

In contrast, WPI-W-W exhibited the least thermal stability, with clear changes in the heat flow profile. A visible endothermic transition around 37 $^{\circ}\text{C}$ might indicate physical changes such as hydration loss, while a weak exothermic peak at $\sim\!44$ $^{\circ}\text{C}$ suggested protein aggregation or matrix rearrangement. These transitions were not reversible upon cooling, implying structural disruption.

By comparison, the other three formulations showed no distinct endothermic or exothermic peaks. Instead, their heat flow curves exhibited smooth, gradual shifts throughout the heating range. This absence of sharp thermal events reflects the lack of abrupt physical transitions such as protein unfolding or network collapse, which may be attributed to enhanced structural integrity and thermal resistance of the emulsion matrix. For reference, ternary emulsions stabilized by chitosan, poly(vinyl alcohol), and poly(lactic acid) exhibited a sharp glasstransition temperature near 57 °C (Grande & Carvalho, 2011), in contrast to the broad, featureless transitions observed in our formulations. Likewise, soy protein hydrolysates-β-glucan-ferulic acid systems showed a well-defined endothermic peak near 56 °C (Jin et al., 2020). These differences suggest that the marine-derived polyphenols in our study may generate less ordered molecular packing at the interface. Possibly caused by their irregular substitution and sulphation patterns, they may disrupt ordered structures and lead to more heterogeneous

X. Duan et al. Food Chemistry 493 (2025) 146011

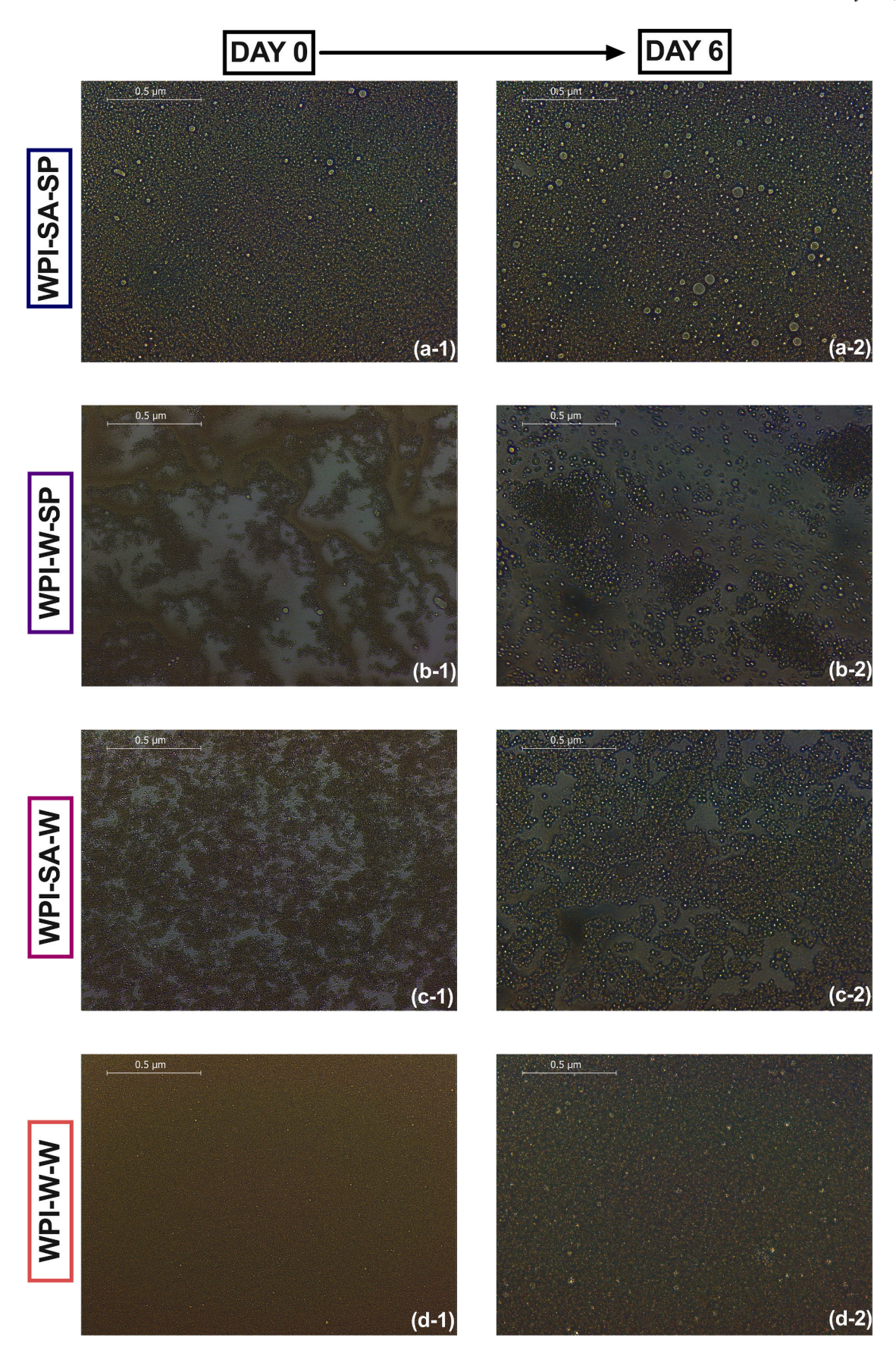


Fig. 2. Optical microscopy images of whey protein isolate-based emulsions at Day 0 and Day 6, respectively. (a-1, b-1, c-1, d-1) Day 0; (a-2, b-2, c-2, d-2) Day 6. Samples are (a) WPI-SA-SP; (b) WPI-W-SP; (c) WPI-SA-W; and (d) WPI-W-W. Magnification: $40 \times /0.65$. Scale bar: 0.5 μ m. WPI, whey protein isolate; SA, sodium alginate; SP, seaweed polyphenol; W, deionized water.

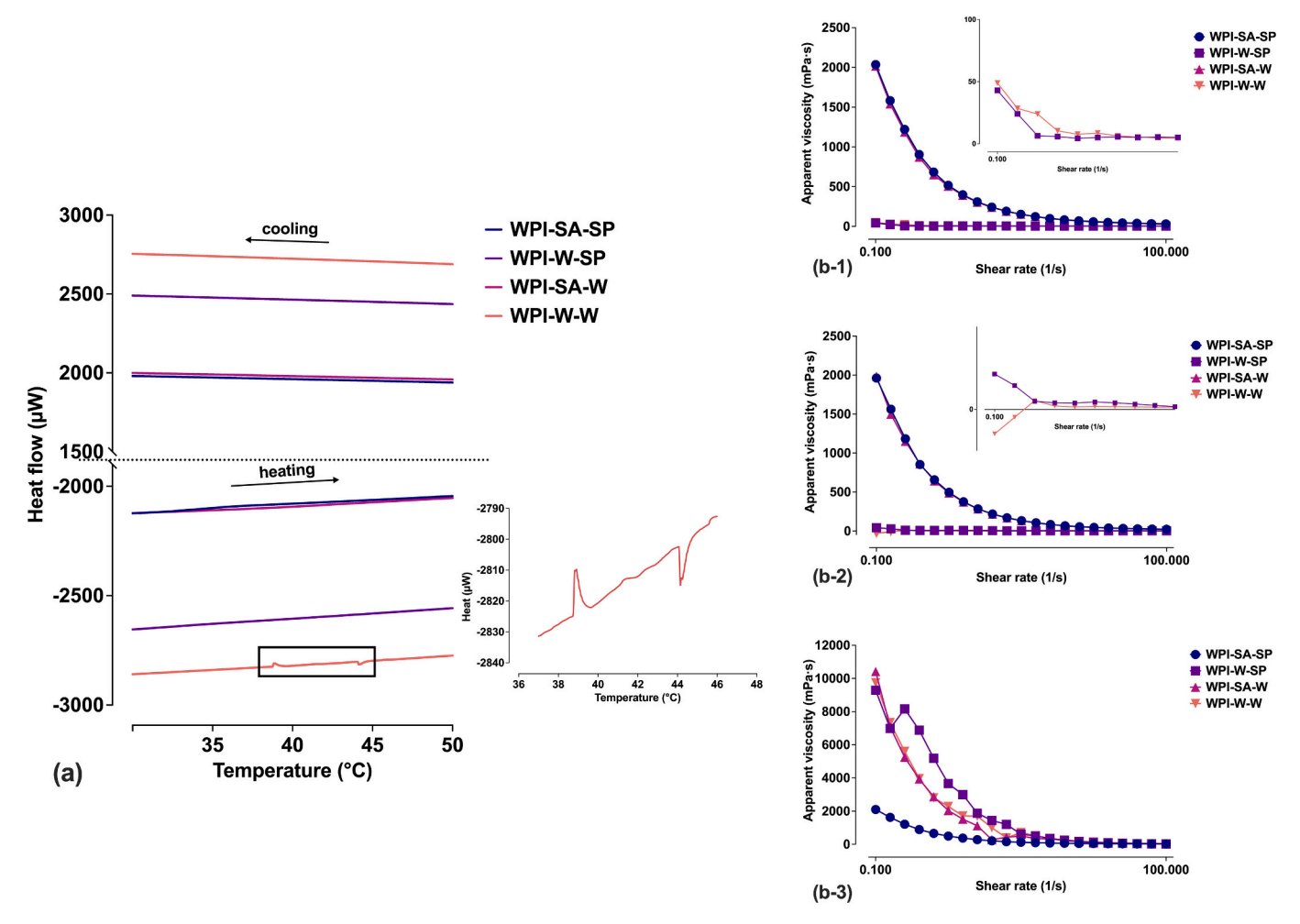


Fig. 3. Thermal and rheological properties of whey protein isolate-based emulsions. (a) Differential scanning calorimetry analysis of heat flow (μ W) during heating and cooling. (b-1) Apparent viscosity (mPa·s) at 4 °C; (b-2) at 25 °C; (b-3) at 37 °C. WPI, whey protein isolate; SA, sodium alginate; SP, seaweed polyphenol; W, deionized water.

thermal behavior.

In the apparent viscosity measurements, only WPI-SA-SP and WPI-SA-W exhibited clear shear-thinning behavior at both 4 °C and 25 °C, whereas WPI-W-SP and WPI-W-W showed negligible changes in viscosity, remaining close to zero mPa·s. The observed shear-thinning (or pseudoplasticity) behavior in the SA-containing systems can be attributed to the presence of SA and SP, which are capable of forming gel-like networks that disintegrate under shear stress, resulting in a decrease in viscosity with increasing shear rate. This response is typical of non-Newtonian fluids with internal structured organization, such as gels or emulsions, where shear disrupts intermolecular interactions and weakens the network (Pal, 2024). In contrast, the nearly Newtonian behavior of WPI-W-SP and WPI-W-W suggested that the interactions within the WPI-only matrix were insufficient to establish a measurable rheological network under the tested conditions or that a comparable gel-like structure was absent. At 37 °C, notable differences emerged; only WPI-SA-SP maintained a relatively stable viscosity at ~2000 mPa·s, which supported the thermal and shear stability of the ternary network. In contrast, the other three formulations experienced a dramatic increase in viscosity, peaking near ~10,000 mPa·s, followed by an abrupt decline with continued shear. The evaluated temperature has favored the unfolding of WPI molecules (Zheng et al., 2014), exposing hydrophobic residues and enhancing heat-induced protein aggregation (Yang et al., 2021), which in turn facilitates the formation of a more extensive protein network and increases viscosity. Additionally, protein-protein interactions may drive droplet flocculation, generating larger droplet clusters that enhance structural resistance and apparent viscosity of emulsions (Fuhrmann et al., 2019). This effect is especially pronounced in emulsions lacking sufficient steric or electrostatic stabilization, such as WPI-W-SP and WPI-W-W.

These findings align with thermal behavior trends observed in DSC analysis. While higher temperatures can induce swelling or gelation in polysaccharide-containing systems, some studies suggested that alginate forms gels independently of temperature, with minimal change in swelling behavior (Pulat & Ozukaya, 2019). In SP-containing systems, elevated temperatures may also trigger polyphenol oxidation, typically occurring above 50–70 °C and affecting compounds like flavonoids and tannins (Antony & Farid, 2022). Oxidized polyphenols can form quinones, which are highly reactive intermediates that covalently bind to proteins through Schiff base formation or Michael addition reactions (Yamaguchi et al., 2022). These covalent interactions enhance protein-polyphenols associations, leading to the development of a stronger interfacial or continuous network, thereby increasing the structural rigidity and apparent viscosity of the emulsion (Jia et al., 2022).

3.1.4. Complex morphological observation

TEM thoroughly examined the morphology of the emulsions at both nanometer and micrometer scales (Fig. 4). In the WPI-SA-SP system, well-defined spherical oil droplets were observed, surrounded by a distinct dark outer layer, consistent with findings reported by Pang et al. (2024). This dark layer was attributed to a network-like structure formed by SA, which increased the viscosity of the continuous phase and

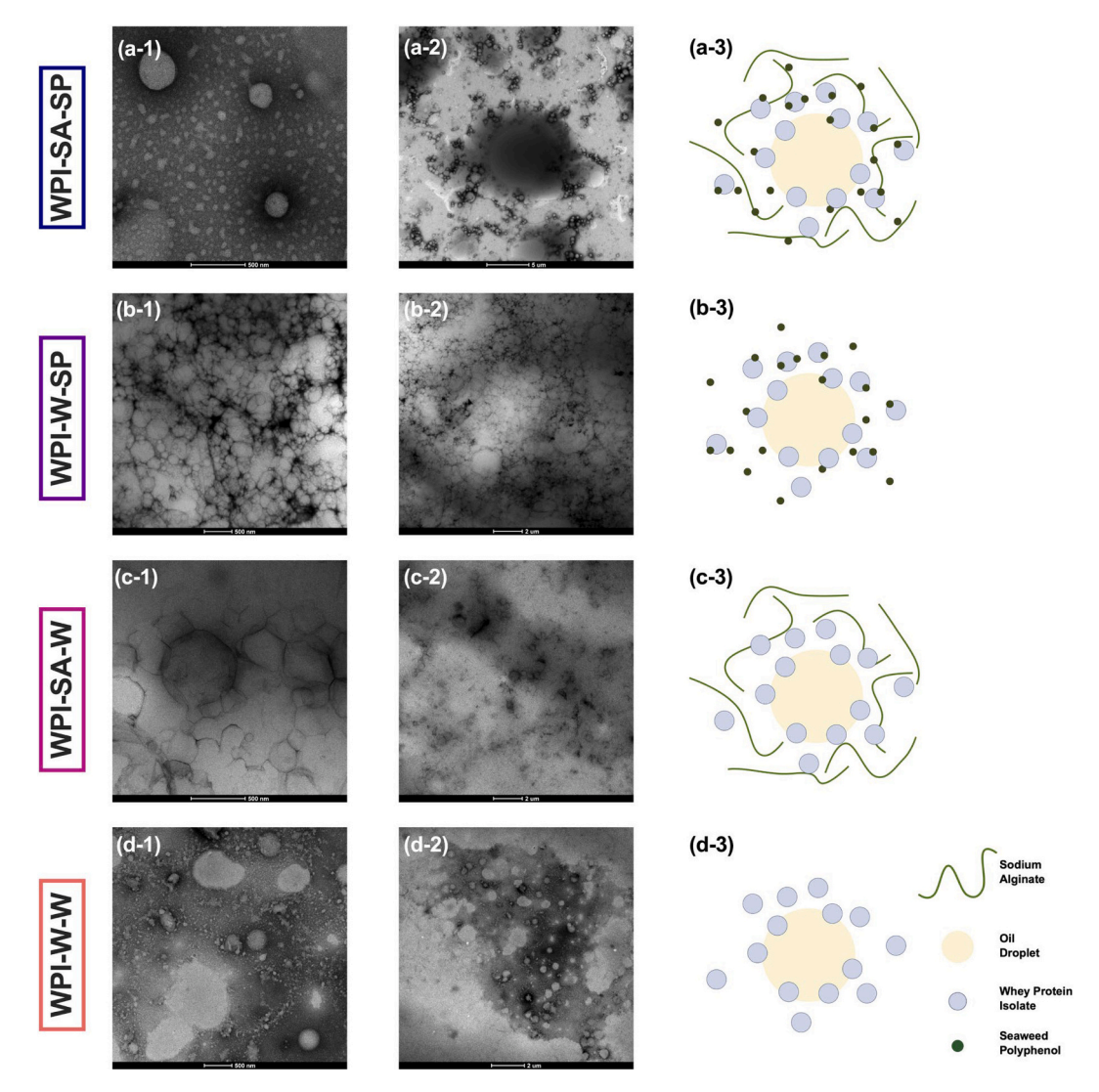


Fig. 4. Transmission electron microscopy images and schematic models of whey protein isolate-based emulsions. (a) WPI-SA-SP; (b) WPI-W-SP; (c) WPI-SA-W; (d) WPI-W-W. Scale bars: (a-1, b-1, c-1, d-1) 500 nm; (a-2) 5 μm; (b-2, c-2, d-2) 2 μm. WPI, whey protein isolate; SA, sodium alginate; SP, seaweed polyphenol; W, dejonized water.

provided steric stabilization. Similar structural behavior has been documented in alginate-stabilized silver nanoparticles (El-Sheekh et al., 2022) and was also evident in the WPI-SA-W emulsion.

WPI played a key role in interfacial stabilization, as evidenced by the characteristic fibrillar morphology seen in the WPI-W-SP system (Cui et al., 2022). Due to the inherent brownish color of SP, the dark fibrous regions observed in TEM images were likely indicative of protein-polyphenol interactions. These may have arisen from hydrogen bonding or covalent cross-linking between the phenolic hydroxyl groups of SP and the amino acid residues of WPI, resulting in localized areas of high electron density. Additionally, SP may have adsorbed onto the protein surface, further enhancing electron scattering. However, the possibility of projection artifacts cannot be excluded entirely.

In contrast, the WPI-W-W system did not exhibit a well-defined emulsion structure, likely due to the exclusive use of WPI as the emulsifier at a relatively low concentration, which may have been insufficient to form a continuous interfacial network. Based on these observations, schematic models were proposed to illustrate the droplet structures and interfacial interactions, consistent with prior studies (Ye et al., 2021).

3.2. In vitro digestion behavior of emulsion formulations

3.2.1. Particle size and ζ-potential

Fig. 5 illustrates the dynamic changes in particle size and ζ -potential of various emulsion formulations throughout simulated gastrointestinal digestion. During the oral phase, all samples exhibited minimal changes in particle size relative to their undigested state, with no statistically significant alterations in 30-min delayed control samples. These results suggest limited structural disruption during oral processing, likely due to the relatively mild physicochemical conditions of the mouth.

Upon transition to the gastric phase, all formulations exhibited a marked increase in particle size, with notable differences between emulsions containing SA and those without. Specifically, SA-containing emulsions displayed a slight increase in particle size during the first hour, rising from 1234.7 \pm 22.95 nm for WPI-SA-SP and 1448.8 \pm 28.21 nm for WPI-SA-W at 0 h, to 1925.2 \pm 18.94 nm and 1617.0 \pm 16.13 nm, respectively, at 1 h. From 1 to 2 h, the particle sizes remained relatively stable. The absence of significant changes in the 3-h control group further supported the cessation of gastric phase activity by that time. The observed increase in particle size can be attributed to controllable flocculation, whereby droplets aggregate without coalescing, preserving microstructural integrity despite apparent

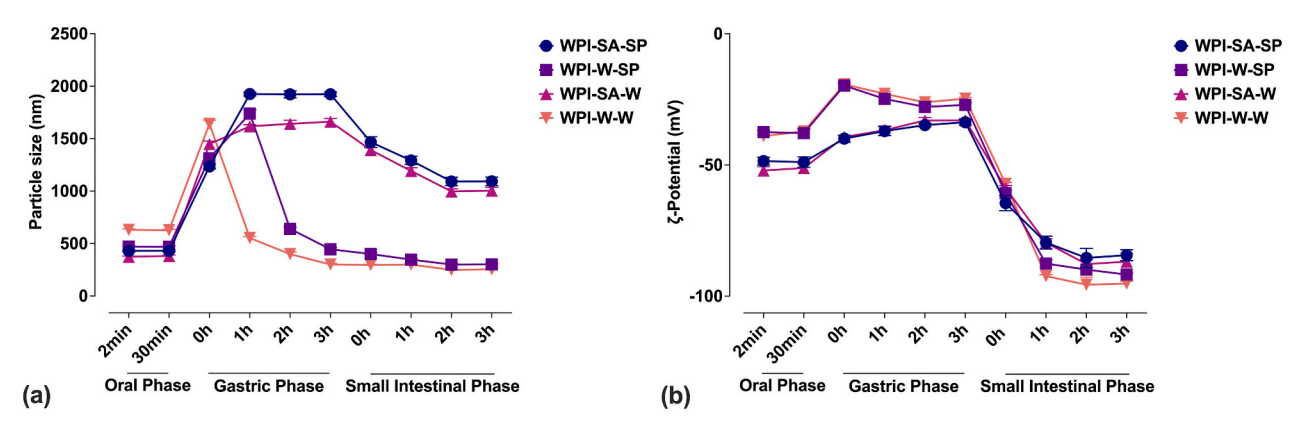


Fig. 5. Changes in (a) particle size (nm) and (b) ζ-potential (mV) of emulsions during in vitro digestion. WPI, whey protein isolate; SA, sodium alginate; SP, seaweed polyphenol; W, deionized water.

macroscopic growth. Wang et al. (2019) similarly reported flocculationinduced growth after 20 min in simulated gastric fluid, from ~1.36 µm to $\sim 211 \, \mu m$, where oil droplets were entrapped within loosely bound protein networks. Rousi et al. (2014) also observed weak flocculation under gastric conditions, attributing this to the pH being significantly above the isoelectric point (pI) of BSA, reducing electrostatic attractions necessary for extensive aggregation. By comparison, SA-free emulsions showed a progressive decline in size, occurring within the first hour for WPI-W-W (from 1642.0 \pm 35.49 nm to 553.8 \pm 12.47 nm) and by the second hour for WPI-W-SP (from 1738.8 \pm 35.49 nm to 640.1 \pm 17.86 nm). The delayed decline of particle size observed in WPI-W-SP compared to WPI-W-W suggested that polyphenol-protein interactions formed a more robust interfacial layer. Polyphenols stabilize protein structures via hydrogen bonding, thus enhancing their resistance to acid-induced denaturation (Xue et al., 2024). Furthermore, polyphenols may reinforce the protein interface by enhancing steric repulsion and viscoelasticity, forming a more cohesive interfacial network (Najari et al., 2024).

During the intestinal phase, particle size reductions were more pronounced in SA-containing emulsions, which suggested a progressive disruption due to bile salts and pancreatic enzymes. Bile salts displaced interfacial proteins and polysaccharides through competitive adsorption, destabilizing droplets and promoting lipid digestion. Additionally, they facilitate lipid solubilization by forming mixed micelles with phospholipids, further displacing original emulsifiers (Sarkar et al., 2016). Nevertheless, SA-containing emulsions (WPI-SA-SP and WPI-SA-W) maintained larger average particle sizes than their SA-free counterparts during the latter intestinal stages, which indicated that the presence of SA imparted some resistance to enzymatic breakdown. Such resistance may be attributed to the formation of a gel-like network at the oil-water interface, limiting access of bile salts and digestive enzymes. Although some studies report that polysaccharides such as cellulose offer limited protection in the intestinal phase (Zhang et al., 2023), others have proposed that robust polysaccharide matrices can hinder digestive diffusion pathways (Sarkar et al., 2018). In addition to the steric and viscoelastic contributions of SA, it is worth noting that divalent cations such as ${\rm Ca}^{2+}$ and ${\rm Mg}^{2+}$, which are naturally present in simulated gastric and intestinal fluids, may have facilitated partial ionic cross-linking of SA chains, forming a weak gel-like network around the droplets. Such ionic interactions could have contributed to delayed structural disruption by limiting the diffusion of bile salts and digestive enzymes into the emulsion core (Haddadzadegan et al., 2022).

For ζ -potential, all emulsion formulations initially exhibited stable, highly negative surface charges in the range of -40 to -50 mV, consistent with their freshly prepared states. This electrostatic stability is characteristic of emulsions stabilized by charged biopolymers and proteins, where repulsive interactions between similarly charged droplets prevent coalescence. Such strong negative potentials reflected

robust electrostatic stabilization under neutral pH conditions.

During the gastric phase, a progressive shift toward less negative ζ -potentials was observed in all samples, decreasing to approximately -20 to -30 mV. This reduction can be attributed to the highly acidic pH and elevated ionic strength of the gastric environment, which compresses the electrical double layer and attenuates electrostatic repulsion among droplets. As reported by Liu et al. (2021) and Wu et al. (2023), the presence of abundant hydrogen ions and monovalent salts in simulated gastric fluids leads to surface charge screening, promoting partial charge neutralization and increasing the likelihood of droplet aggregation.

Among the formulations, WPI-W-SP exhibited the most pronounced charge neutralization, suggesting a heightened susceptibility of its interfacial structure to gastric destabilization. A potential explanation is a unique interaction between WPI and polyphenols, whereby the resulting complexes exhibit altered charge responsiveness under acidic conditions. In contrast, formulations containing SA (WPI-SA-SP and WPI-SA-W) maintained a relatively more stable ζ -potential profile. This stabilization is likely due to the polyelectrolyte nature of SA, which can provide buffering capacity and steric hindrance that protect the interfacial layer from extensive charge alteration. Similar electrostatic shielding effects have been reported in previous studies where fucoidan-sodium caseinate emulsions retained surface charge integrity during simulated gastric digestion (Zhang et al., 2025).

Transitioning into the small intestinal phase, all samples experienced a dramatic shift toward highly negative ζ-potentials, primarily driven by the adsorption of bile salts. These amphiphilic molecules, predominantly anionic at intestinal pH, rapidly adsorb to the oil-water interface, forming a dense, negatively charged interfacial layer (Shen et al., 2024; Wang et al., 2019). Additionally, the accumulation of digestion products, such as peptides, fatty acids, and monoacylglycerols, can further enhance the negative surface charge (Liu et al., 2021). The WPI-W-SP formulation demonstrated an especially pronounced drop, reaching nearly -90 mV, suggesting an improved capacity for bile salt binding. The interaction between SP and bile salt micelles may explain this observation. Polyphenols have been reported to modify interfacial properties and potentially enhance bile salt affinity through hydrogen bonding or hydrophobic interactions (Naumann et al., 2020). Thus, the presence of SP could have facilitated tighter bile salt packing at the interface, amplifying the negative surface potential. The elevated pH of the small intestinal environment (pH \sim 7.0–7.5) also plays a critical role, promoting the complete deprotonation of ionizable groups on both proteins and polysaccharides, thereby restoring or intensifying the negative surface charge (Zhang et al., 2015).

3.2.2. Chemical composition

The concentration of total phenolic compounds, protein, and uronic acid throughout the simulated digestion process was summarized in

Food Chemistry 493 (2025) 146011

Table 2Changes in chemical composition of emulsion systems during in vitro digestion.

	Oral Phase			Gastric Phase					Small Intestinal Phase							
	2 min	30 min	Positive Control	Negative Control	0 h	1 h	2 h	3 h	Positive Control	Negative Control	0 h	1 h	2 h	3 h	Positive Control	Negative Control
Total phenoli	c content (mg	GAE/g)														
WPI-SA-SP	$\begin{array}{l} 0.00 \; \pm \\ 0.01^{cE} \end{array}$	$\begin{array}{l} 0.00 \; \pm \\ 0.04^{bE} \end{array}$	$\begin{array}{l} 0.01 \pm \\ 0.12^{bcDE} \end{array}$		$\begin{array}{l} 0.41 \pm \\ 0.07^{bBC} \end{array}$	0.34 ± 0.04^{bC}	$\begin{array}{l} 0.58 \pm \\ 0.06^{abABC} \end{array}$	0.75 ± 0.05^{aA}	$\begin{array}{l} 0.37 \pm \\ 0.05^{aBC} \end{array}$		$\begin{array}{l} 0.77 \pm \\ 0.08^{aA} \end{array}$	$\begin{array}{l} 0.39 \pm \\ 0.13^{bBC} \end{array}$	$\begin{array}{l} 0.31 \pm \\ 0.07^{bCD} \end{array}$	$\begin{array}{l} 0.41 \pm \\ 0.26^{aBC} \end{array}$	$\begin{array}{l} 0.67 \pm \\ 0.09^{aAB} \end{array}$	
WPI-W-SP	$\begin{array}{l} 0.23 \pm \\ 0.03^{aBC} \end{array}$	$\begin{array}{l} 0.18 \pm \\ 0.04^{aC} \end{array}$	$\begin{array}{l} 0.32 \pm \\ 0.04^{aABC} \end{array}$		$\begin{array}{l} 0.68 \pm \\ 0.14^{aA} \end{array}$	$\begin{array}{l} 0.64 \pm \\ 0.11^{aA} \end{array}$	$\begin{array}{l} 0.39 \pm \\ 0.13^{\mathrm{bABC}} \end{array}$	$\begin{array}{l} 0.42 \pm \\ 0.19^{bABC} \end{array}$	$\begin{array}{l} 0.18 \pm \\ 0.20^{aC} \end{array}$		$\begin{array}{l} 0.64 \pm \\ 0.10^{abA} \end{array}$	$\begin{array}{l} 0.69 \pm \\ 0.09^{aA} \end{array}$	$\begin{array}{l} 0.56 \pm \\ 0.04^{aABC} \end{array}$	$\begin{array}{l} 0.61 \pm \\ 0.13^{aAB} \end{array}$	$\begin{array}{l} 0.35 \pm \\ 0.27^{aABC} \end{array}$	
WPI-SA-W	$\begin{array}{c} 0.00 \; \pm \\ 0.03^{\text{cCD}} \end{array}$	$\begin{array}{l} 0.02 \pm \\ 0.13^{abCD} \end{array}$	$\begin{array}{c} 0.00 \pm \\ 0.05^{\text{cCD}} \end{array}$		$\begin{array}{l} 0.35 \pm \\ 0.04^{bAB} \end{array}$	$\begin{array}{l} \textbf{0.40} \pm \\ \textbf{0.08}^{\text{bAB}} \end{array}$	$\begin{array}{l} 0.52 \pm \\ 0.37^{abA} \end{array}$	$\begin{array}{l} 0.48 \pm \\ 0.07^{abA} \end{array}$	$\begin{array}{l} 0.16 \pm \\ 0.05^{aBC} \end{array}$		$\begin{array}{l} 0.38 \pm \\ 0.20^{bAB} \end{array}$	$\begin{array}{l} 0.31 \pm \\ 0.04^{bAB} \end{array}$	$\begin{array}{c} 0.00 \pm \\ 0.09^{\text{cCD}} \end{array}$	$\begin{array}{c} 0.00 \pm \\ 0.17^{bCD} \end{array}$	$\begin{array}{l} 0.12 \pm \\ 0.03^{\text{cBC}} \end{array}$	
WPI-W-W	$\begin{array}{c} 0.08 \pm \\ 0.02^{bCD} \end{array}$	$\begin{array}{l} 0.04 \pm \\ 0.02^{abD} \end{array}$	$\begin{array}{c} 0.01 \pm \\ 0.06^{\mathrm{bD}} \end{array}$		$\begin{array}{l} 0.77 \; \pm \\ 0.08^{aA} \end{array}$	$\begin{array}{l} 0.67 \pm \\ 0.18^{aA} \end{array}$	$\begin{array}{l} 0.76 \pm \\ 0.10^{aA} \end{array}$	$\begin{array}{l} 0.75 \pm \\ 0.14^{aA} \end{array}$	$\begin{array}{l} 0.17 \pm \\ 0.11^{aBCD} \end{array}$		$\begin{array}{l} 0.35 \pm \\ 0.12^{bB} \end{array}$	$\begin{array}{l} 0.36 \pm \\ 0.10^{bB} \end{array}$	$\begin{array}{l} 0.30~\pm\\ 0.02^{bBC} \end{array}$	$\begin{array}{l} 0.35 \pm \\ 0.07^{abB} \end{array}$	$\begin{array}{l} 0.12 \pm \\ 0.05^{abBCD} \end{array}$	
Negative Control				0.00 ± 0.00						$\begin{array}{c} 0.05 \pm \\ 0.02 \end{array}$						0.99 ± 0.09
Protein conte	nt (mg/g) 0.00 ±	$0.00 \pm$	$0.00 \pm$		$1.22~\pm$	$0.63 \pm$	$0.68 \pm$	$0.72~\pm$	$1.22~\pm$		7.01 \pm	8.32 \pm	6.93 ±	6.64 ±	2.11 \pm	
WPI-SA-SP	0.17^{bF}	0.02^{bF}	0.35^{bF}		$0.21^{\rm cCD}$	0.11^{cDE}	$0.08 \pm 0.07^{\text{cDE}}$	0.17^{bDE}	0.16^{bCD}		0.86 ^{abB}	0.39^{aA}	0.24 ^{aB}	0.18 ^{aB}	0.35^{bC}	
WPI-W-SP	1.58 ± 0.02^{aEF}	1.44 ± 0.06^{aEF}	$1.22 \pm \\ 0.25^{aEF}$		$1.84 \pm 0.36^{ m bE}$	$\begin{array}{c} 1.02 \pm \\ 0.24^{\mathrm{bF}} \end{array}$	$\begin{array}{c} 1.17 \pm \\ 0.09^{\mathrm{bEF}} \end{array}$	$\begin{array}{l} 0.82 \pm \\ 0.22^{\mathrm{bF}} \end{array}$	$\begin{array}{c} 2.65 \pm \\ 0.12^{\text{aD}} \end{array}$		$\begin{array}{l} \textbf{6.74} \pm \\ \textbf{0.22}^{\text{bA}} \end{array}$	$6.32 \pm 0.39^{\mathrm{bA}}$	$6.07 \pm \\ 0.39^{bcAB}$	$5.54 \pm 0.17^{ m bB}$	4.29 ± 0.41^{aC}	
WPI-SA-W	$0.00 \pm 0.29^{ m bF}$	$\begin{array}{l} 0.00 \pm \\ 0.16^{\mathrm{bF}} \end{array}$	$0.00 \pm 0.48^{\mathrm{bF}}$		$\begin{array}{c} 1.05 \pm \\ 0.07^{\text{cD}} \end{array}$	$\begin{array}{l} 0.51 \pm \\ 0.13^{\text{cDEF}} \end{array}$	$\begin{array}{c} 0.65 \pm \\ 0.10^{\text{cDE}} \end{array}$	$\begin{array}{c} 1.02 \pm \\ 0.08^{abD} \end{array}$	$0.98 \pm 0.04^{ m bD}$		$\begin{array}{l} 8.15 \pm \\ 0.20^{aA} \end{array}$	8.96 ± 0.71^{aA}	$\begin{array}{l} 6.86 \pm \\ 0.13^{abB} \end{array}$	6.75 ± 0.59^{aB}	2.09 ± 0.03^{bC}	
WPI-W-W	$\begin{array}{c} 1.12 \pm \\ 0.20^{aF} \end{array}$	$\begin{array}{l} 1.10 \; \pm \\ 0.25^{aF} \end{array}$	$\begin{array}{c} 1.21 \pm \\ 0.07^{aF} \end{array}$		$\begin{array}{c} 2.93 \pm \\ 0.27^{aD} \end{array}$	$\begin{array}{l} 1.98 \pm \\ 0.22^{aE} \end{array}$	$1.68 \pm \\ 0.07^{aEF}$	$\begin{array}{l} 1.38 \pm \\ 0.09^{aEF} \end{array}$	0.02 ± 0.49^{cG}		$\begin{array}{c} 6.83 \pm \\ 0.10^{\mathrm{bA}} \end{array}$	$\begin{array}{l} \textbf{5.87} \pm \\ \textbf{0.10}^{\text{bB}} \end{array}$	5.78 ± 0.42^{cB}	$\begin{array}{l} \textbf{5.48} \pm \\ \textbf{0.32}^{\text{bB}} \end{array}$	$\begin{array}{l} 3.83 \pm \\ 0.18^{\text{aC}} \end{array}$	
Negative Control Uronic acid c	content (mg/g)		0.43 ± 0.02						0.00 ± 0.04						4.63 ± 0.13
WPI-SA-SP	6.59 ± 0.28 ^{bEF}	$7.26 \pm 0.26^{ m aDE}$	$\begin{array}{l} 6.72 \pm \\ 0.28^{\mathrm{bEF}} \end{array}$		$\begin{array}{c} 8.51 \pm \\ 0.23^{aCD} \end{array}$	$\begin{array}{l} 6.79 \pm \\ 0.31^{aEF} \end{array}$	$7.53 \pm \\ 0.12^{abCDE}$	$\begin{array}{l} \textbf{7.47} \pm \\ \textbf{0.40}^{\text{aCDE}} \end{array}$	$\begin{array}{c} 8.80 \; \pm \\ 0.45^{aC} \end{array}$		$7.19 \pm \\ 0.29^{\text{bDE}}$	$12.93 \pm 1.41^{\text{bA}}$	$13.30 \pm \\ 0.47^{aA}$	11.28 ± 0.35^{abB}	5.71 ± 0.30^{cF}	
WPI-W-SP	6.55 ± 0.24^{bG}	$^{4.64~\pm}_{0.24^{ m bH}}$	$6.16 \pm 0.61^{\mathrm{bG}}$		$\begin{array}{c} 8.77 \pm \\ 0.20^{aDE} \end{array}$	6.79 ± 0.16^{aFG}	$\begin{array}{l} 7.09 \pm \\ 0.50^{bFG} \end{array}$	7.41 ± 0.06^{aFG}	9.13 ± 0.30^{aCD}		$\begin{array}{c} \textbf{7.85} \pm \\ \textbf{0.28}^{abEF} \end{array}$	15.17 ± 0.61^{aA}	$10.15 \pm 0.71^{ m bBC}$	$11.11 \pm 0.68^{\text{abB}}$	$\begin{array}{l} 6.32 \pm \\ 0.17^{bcG} \end{array}$	
WPI-SA-W	5.01 ± 0.09^{cF}	5.04 ± 0.38 ^{bF}	6.99 ± 0.24 ^{bDE}		9.03 ± 0.23 ^{aB}	$6.32 \pm \\ 0.17^{\text{aDE}}$	$\begin{array}{l} 8.22 \pm \\ 0.36^{\mathrm{aBC}} \end{array}$	$5.81 \pm 0.36^{\mathrm{bEF}}$	$6.37 \pm 0.39^{\text{bDE}}$		8.72 ± 0.51^{abB}	9.06 ± 0.35 ^{cB}	11.60 ± 0.82^{abA}	$10.88 \pm 0.28^{\mathrm{bA}}$	7.32 ± 0.58^{abCD}	
WPI-W-W	7.94 ± 0.54 ^{aEF}	$7.03 \pm \\ 0.27^{aFG}$	8.44 ± 0.59 ^{aDE}		$6.14 \pm \\ 0.28^{\mathrm{bGH}}$	5.34 ± 0.30 ^{bHI}	$5.10 \pm 0.24^{ m cIJ}$	4.91 ± 0.49 ^{bJ}	$5.92 \pm 0.19^{ m bHI}$		$9.38 \pm 1.00^{ m aD}$	11.98 ± 0.36 ^{bB}	10.97 ± 0.57^{bC}	13.12 ± 1.30 ^{aA}	7.69 ± 0.37 ^{aEF}	
Negative Control				0.00 ± 0.02						0.03 ± 0.13						20.51 ± 0.20

Data are presented as mean \pm standard deviation (n=3). Lowercase letters (a-c) indicate significant differences between samples at the same time point, while uppercase letters (A-J) denote significant differences within each sample across different time points. Component contents were calculated separately. Statistical significance (p<0.05) was determined by one-way analysis of variance (ANOVA) followed by Tukey's multiple comparison test. Negative control refers to deionized water mixed with digestive fluids; positive control refers to sample mixed with deionized water. GAE, gallic acid equivalent; WPI, whey protein isolate; SA, sodium alginate; SP, seaweed polyphenol; W, deionized water.

Table 2. Across all four formulations, the TPC remained relatively low and nearly undetectable during the oral phase (0.00-0.32 mg GAE/g), likely due to the strong molecular interactions, such as hydrogen bonding and hydrophobic associations between polyphenols and the emulsion matrix, which restricted their release and limited detectability under the mild conditions of the oral phase. Upon entry into the gastric phase, a notable increase in TPC was observed across all samples (~ 0.34–0.77 mg GAE/g), including those not originally containing added polyphenols. This unexpected rise in TPC for SP-free formulations may be attributed to interference from other gastric digestion products that can also react with the Folin-Ciocalteu reagent, such as peptides, amino acids, or lipid oxidation products, resulting in a positive TPC signal. The increase in TPC observed within this phase in SP-containing formulations can be primarily attributed to the acid-induced denaturation and enzymatic hydrolysis of protein-polyphenol complexes. Similar findings were reported by Chen et al. (2019), who observed an increased bioaccessible amount of phenolic compounds after two hours of gastric digestion (from 20.4 to 24.3 mg GAE/g). Under gastric conditions, the unfolding of WPI structures exposes and releases polyphenols that were previously bound or entrapped within the emulsion matrix. In addition, the partial breakdown of SA scaffolds may contribute to the gradual diffusion of SP into the surrounding fluid. The disruption of polyphenolprotein or polyphenol-polysaccharide networks under acidic pH and pepsin action thereby enhances the measurable release of phenolic

Protein content followed a trend similar to that of phenolic compounds. In the oral and early gastric phases, protein concentrations remained low (0.00-1.58 mg/g), indicating the formation of stable emulsion structures in which proteins functioned primarily as interfacial stabilizers. At this stage, a significant portion of the protein was still embedded within the emulsion interface or internal matrix and thus not readily detectable in the aqueous phase. However, a slight increase in protein concentration was observed during the gastric phase (0.51-2.93 mg/g). Among all samples, the protein concentration of WPI-W-W exhibited the highest increase (almost twofold). This rise can be attributed to two main factors: a) protein denaturation and b) structural loosening of the emulsion system. Under acidic gastric conditions, the tertiary and secondary structures of proteins unfold, exposing hydrophobic and charged residues, thereby increasing solubility and detectability. Furthermore, the presence of pepsin initiates proteolytic cleavage of proteins, producing smaller peptide fragments that are more readily solubilized (Yang et al., n.d.). The breakdown of the interfacial structure also facilitated the release of previously entrapped proteins into the gastric fluid. Collectively, these changes reflect the onset of protein destabilization and release from the emulsion matrix, with the emulsion WPI-W-W the most unstable. In the small intestinal phase, protein concentration increased even more significantly (up to 8.15 mg/ g, p < 0.05). This escalation is primarily due to the secretion of pancreatic proteases (e.g., trypsin, chymotrypsin, and carboxypeptidase), which further degrade proteins into smaller peptides and amino acids. These enzymes, being proteins themselves, also contribute to the total measurable protein content in the system. Moreover, bile salts aid in disrupting the emulsion structure and emulsifying lipids, which in turn promotes the release of proteins previously enclosed within oil droplets. The progressive enzymatic hydrolysis temporarily elevates protein concentration in the intestinal fluid before eventual absorption by the intestinal epithelium. These observations are consistent with the findings of Garcia-Campayo et al. (2018), who reported similar increases in protein solubilization and breakdown during in vitro gastrointestinal digestion.

The uronic acid content continuously increased throughout the entire digestion process, which proved a progressive release and solubilization of SA or its degradation products from the emulsion matrix. In the gastric phase, although the low pH typically promotes SA gelation by converting carboxylate groups into their protonated form and forming insoluble alginic acid (Frent et al., 2022), a gradual loosening of the gel

network may still occur. For example, Bhansali et al. (2021) mentioned that the alginate matrix is prone to cracking at lower pH (stomach), which may trigger the structural burst. Several factors, such as ionic exchange and structural disruption caused by pepsin activity, all of which allow limited diffusion of uronic acid into the gastric fluid. The opposite opinion was proposed by Geng et al. (2024), who found that SA-hydrogel beads shrank under the acidic conditions formed by the gastric juice, which improved their mechanical strength and structural density, thus preventing bead structure collapse and limiting diffusion through the matrix. The increase became more pronounced in the intestinal phase, the presence of bile salts likely disrupted the gel matrix through emulsification and competitive binding interactions, enhancing the release of uronic acid residues (Wang et al., 2001). Although sodium alginate is relatively resistant to enzymatic degradation, prolonged exposure to intestinal conditions has further facilitated the disintegration of the alginate network. Together, these factors contributed to the sustained increase in uronic acid concentration over time, reflecting the gradual breakdown and release of the polysaccharide from the emulsion structure during digestion. In a study related to emulsion-alginate beads, almost all samples showed disintegrative behavior under intestinal conditions (Wu et al., 2024). To the best of our knowledge, this is the first study to simultaneously monitor the compositional changes of all three key emulsion components during simulated gastrointestinal digestion, which offered new insights into the behavior and stability of complex emulsions.

3.2.3. Antioxidant capacity

The radical scavenging capacity of emulsion systems during their digestion process was determined using DPPH and •OH radicals, with trends of each sample shown in Fig. 6. In general, the freshly made WPI-SA-SP and WPI-W-SP emulsions exhibited higher antioxidant activity than the other two formulations, owing to the presence of SP, which contributed polyphenolic compounds with radical-scavenging ability. However, the overall activity remained limited at the initial stage, due to the encapsulation of polyphenols within the emulsion cores. •OH scavenging was slightly higher than DPPH in all cases.

During digestion, WPI-SA-SP showed a slight decrease in antioxidant capacity during the oral phase (~40 %), followed by a modest increase in the gastric environment (up to 58.2%), and a marked rise in the early small intestinal phase (up to 85.7% within the first hour). Similar to the results reported by Shen et al. (2024), a significant decrease in the scavenging capacity of casein-caffeic acid-glucose ternary conjugates was observed, which was explained by the hydrolysis of the protein-based emulsifier surrounding the droplets and structural damage caused by pepsin and the low pH environment. This trend corresponded with our TPC results, which showed that the gradual release of polyphenols from the WPI-SA-SP systems across the gastrointestinal phase reached a peak when entering the intestinal phase (0.77 \pm 0.08 mg/g) and then declined. The viscoelastic and multilayer interfacial structure formed by SA-WPI conjugates may have delayed the release of SP and contributed to a controlled release profile.

A different pattern was observed in the WPI-W-SP system, where antioxidant activity markedly increased during the early gastric phase, reaching 74.2 % at 2 h, before declining to 53.2 % by the end of gastric digestion (3 h) and continuing to decrease during the small intestinal phase, reaching 27.6 % at 3 h. In the oral phase, SP's radical-scavenging activity was suppressed due to its binding with WPI, which limited its immediate availability; however, acid-induced structural changes during gastric digestion facilitated the release of bound polyphenols, thereby enhancing their antioxidant activity. Partial hydrolysis of the protein matrix by pepsin may have exposed additional reactive sites or liberated active polyphenol forms, contributing to the observed early gastric increase. As digestion progressed, the continued breakdown of polyphenols or their prior reactions with free radicals likely led to the subsequent decline in activity.

Additionally, phenolic compounds are generally unstable under

X. Duan et al. Food Chemistry 493 (2025) 146011

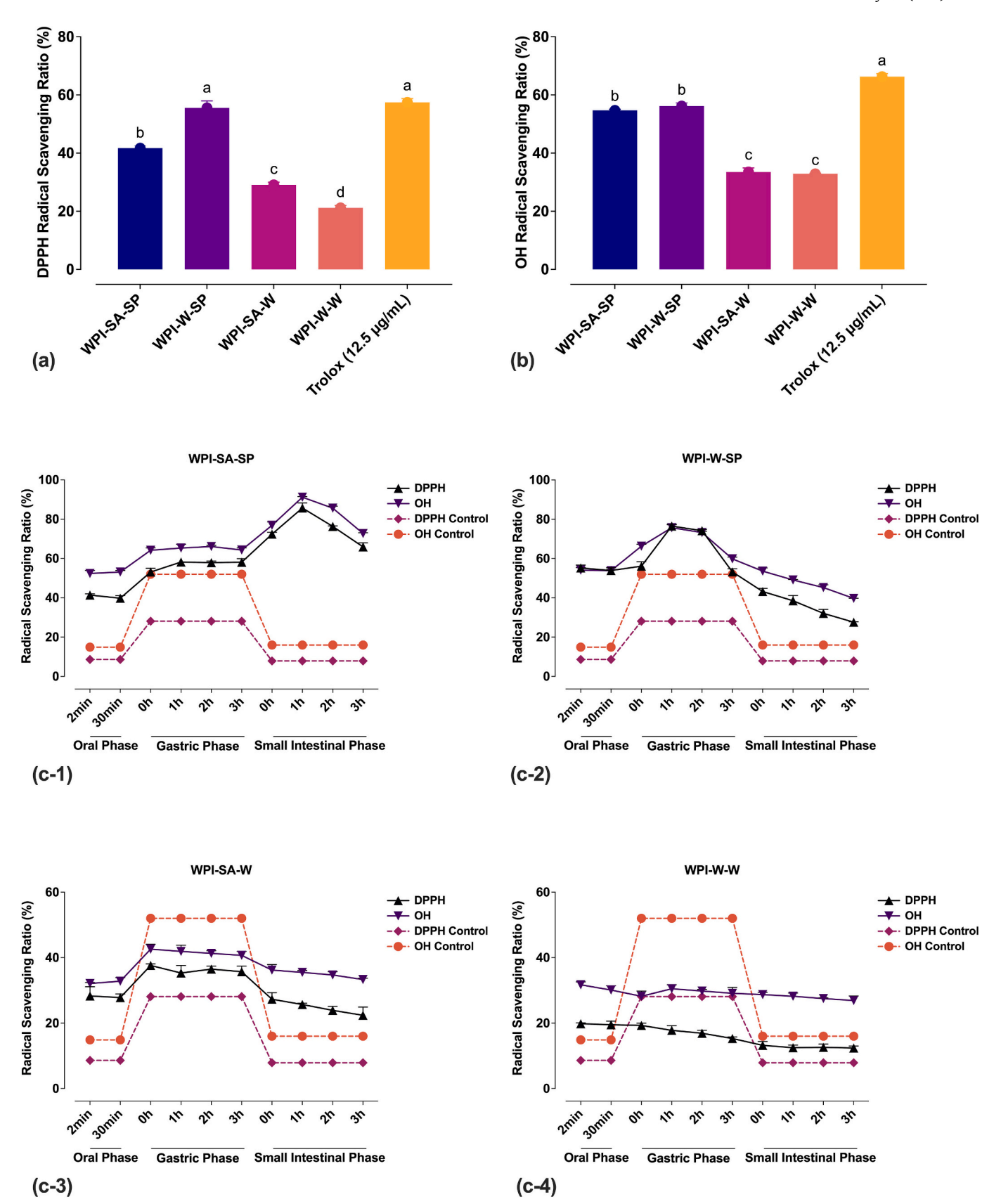


Fig. 6. Antioxidant activity of whey protein isolate-based emulsions. (a) DPPH and (b) hydroxyl radical (\bullet OH) scavenging abilities (%) of undigested emulsions (Trolox used as standard). Lowercase letters indicate significant differences between different samples (p < 0.05). (a-d) (c-1 to c-4) Radical scavenging abilities (%) of digested emulsions for WPI-SA-SP, WPI-W-SP, WPI-SA-W, and WPI-W-W, respectively. WPI, whey protein isolate; SA, sodium alginate; SP, seaweed polyphenol; W, deionized water.

alkaline conditions, and previous studies have reported polyphenol oxidation in such environments (Kim et al., 2025), which may explain the reduced electron-donating capacity observed in the intestinal phase. The addition of pancreatin and bile salts further disrupted the emulsion structure, leading to droplet coalescence and phase separation. This structural breakdown reduced the interfacial area where SP was concentrated and active. Although proteolysis by pancreatic enzymes facilitated the release of previously protein-bound polyphenols, these compounds may have rapidly interacted with other digestive components, such as bile salts, thereby decreasing their availability as radical scavengers.

In emulsions lacking SP, the continuous decline in antioxidant activity suggested that any inherent antioxidant properties were progressively lost during digestion. This is probably due to the gradual hydrolysis of WPI by digestive enzymes, which may have disrupted its tertiary structure and diminished its natural antioxidant functionality. In parallel, the breakdown of the emulsion matrix increased lipid exposure to the aqueous phase, potentially accelerating oxidative degradation and further reducing antioxidant capacity.

Although SA can form protective gels under acidic conditions, which may shield antioxidant compounds from degradation, its molecular mobility in the gel state is reduced (Degrassi et al., 1998). As a result, antioxidant functional groups (e.g., carboxyl and hydroxyl moieties) are less exposed and thus less reactive toward free radicals, ultimately limiting overall antioxidant efficacy.

3.2.4. Free fatty acid release

The kinetics of FFA release are shown in Fig. 7. During the gastric phase, the WPI-SA-W and WPI-SA-SP formulations exhibited strong resistance to lipolysis, with FFA release remaining below 10 % throughout the three-hour incubation. This remarkable gastric protection is consistent with the well-documented ability of SA to form an acid-induced, insoluble gel matrix that limits enzyme diffusion and access to encapsulated lipids (Li et al., 2011). They also reported that the rate of the enzymes will depend on the pore size of this gel network and on any specific interactions of the enzyme with the molecules that comprise the gel network (e.g., electrostatic or hydrophobic interactions). The formation of a protein-polysaccharide network between WPI and SA may have further reinforced this barrier, contributing to the minimal lipase

activity observed in these systems.

In contrast, formulations lacking SA (WPI-W-W and WPI-W-SP) showed significantly higher FFA release (p < 0.05) starting from the gastric phase. WPI-W-W reached ~55 % FFA release, while WPI-W-SP reached ~40 % after 3 h. This trend aligns with the findings of Velderrain-Rodríguez et al. (2023), κ-carrageenan or agar reduced final FFA release to 44 % and 55 %, respectively, compared with 70 % in emulsions without polysaccharides after 20 min of intestinal digestion. Such reductions are generally attributed to the formation of interfacial or network barriers that restrict enzyme access. Rigid gels formed by κ/ι-carrageenan, konjac glucomannan, SA, and low acyl gellan can withstand gastrointestinal shear. As a result, they slow lipid hydrolysis and delay the release of encapsulated lipophilic compounds (Khin et al., 2021). In our system, the presence of marine polyphenols may further reinforce these barriers through protein-polysaccharide-polyphenol cross-linking. In contrast, cellulose nanocrystals in pea-protein microgel emulsions increased final FFA release by 2–5 % (Zhang et al., 2023). The authors explained this effect by the greater oil droplet surface area generated after gastric breakdown, which facilitated enzyme action.

A dramatic shift in FFA release was observed upon transition to the intestinal phase. The most striking change occurred in WPI-SA-W, where FFA release increased abruptly from $\sim\!5$ % to 60% within the first hour of exposure to intestinal fluid. This rapid release could be attributed to the pH-sensitive solubilization of the SA gel matrix, which shifted to alkaline conditions, thus exposing lipids to pancreatic enzymes. By the end of the intestinal phase, WPI-W-W and WPI-W-SP achieved the highest final FFA release ($\sim\!70$ %), indicating nearly complete lipid digestion. In contrast, WPI-SA-W and WPI-SA-SP plateaued at slightly lower values ($\sim\!55$ –60%). Interactions between polysaccharides and bile salts may impede lipid digestion by reducing bile salt adsorption at the oil–water interface, thereby limiting lipase accessibility and enzymatic hydrolysis (Klinkesorn & Julian McClements, 2010).

4. Conclusion

In this study, a novel ternary emulsion system composed of WPI, SA, and SP was successfully prepared via high-pressure homogenization. The emulsions showed a small average droplet size (428.8 \pm 5.4 nm) and a highly negative $\zeta\text{-potential}$ (–47.1 \pm 1.1 mV), which indicated

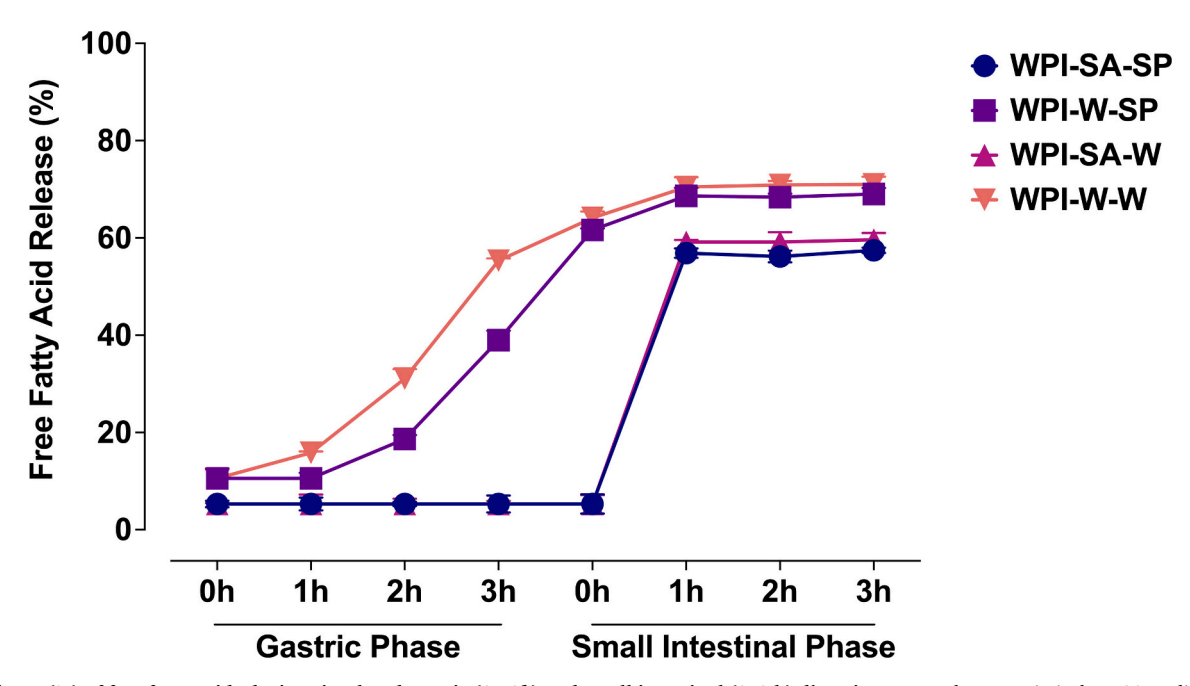


Fig. 7. Release (%) of free fatty acids during simulated gastric (0-3h) and small intestinal (0-3 h) digestion. WPI, whey protein isolate; SA, sodium alginate; SP, seaweed polyphenol; W, deionized water.

X. Duan et al. Food Chemistry 493 (2025) 146011

excellent colloidal stability. Physicochemical analyses demonstrated that the ternary system had stable thermal properties and did not show physical change compared to emulsions stabilized by WPI alone. The emulsions exhibited beneficial non-Newtonian rheological behavior with an apparent viscosity consistently around 2000 mPa·s across different temperatures, which supported their stability and texture. Under simulated gastrointestinal digestion, the ternary emulsions inhibited FFA release more effectively than binary and singlecomponent systems. Approximately 15 % less free fatty acid was released in the intestinal phase, and no significant release occurred in the gastric phase. The antioxidant capacity of the ternary system in the intestinal phase was twice that of the binary emulsions and more than three times higher than emulsions stabilized only by WPI. These results showed that SA acted as a protective matrix against enzymatic breakdown, while SP improved antioxidant capacity and interfacial stability through synergistic effects with the other components. In summary, the WPI-SA-SP ternary complex exhibited superior structural stability, controlled lipid digestion, and enhanced antioxidant function. This system has strong potential for applications as an effective delivery vehicle in functional foods and nutraceuticals.

CRediT authorship contribution statement

Xinyu Duan: Writing – original draft, Methodology, Investigation, Formal analysis, Data curation, Conceptualization. Cundong Xie: Writing – review & editing, Methodology. Muthupandian Ashokkumar: Writing – review & editing, Supervision, Conceptualization. Frank R. Dunshea: Writing – review & editing, Supervision, Conceptualization. Hafiz A.R. Suleria: Writing – review & editing, Validation, Supervision, Resources, Investigation, Funding acquisition, Conceptualization.

Funding

The research was funded by the Australian Research Council under the "Discovery Early Career Award" (Grant No. ARC-DECRA-DE220100055) and the University of Melbourne under the "Collaborative Research Development Grant" (Grant No. UoM-21/23).

Declaration of competing interest

The authors declare that they have no known competing financial interests or personal relationships that could have appeared to influence the work reported in this paper.

Acknowledgements

We would like to thank the Ian Holmes Imaging Centre and Melbourne Protein Characterization Facility of the Bio21 Molecular Science and Biotechnology Institute at the University of Melbourne for their support throughout this study.

Data availability

Data will be made available on request.

References

- Antony, A., & Farid, M. (2022). Effect of temperatures on polyphenols during extraction. Applied Sciences, 12(4), 2107. https://doi.org/10.3390/app12042107
- AOCS, A. O. C. S. (2017). Official method cd 3d-63: Acid value. In M. W. Collison (Ed.), Official methods and recommended practices of the AOCS (7th edition ed.). American Oil Chemists Society.
- Bhansali, M., Dabholkar, N., Swetha, P., Dubey, S. K., & Singhvi, G. (2021). Chapter 18-solid Oral controlled-release formulations. In A. T. Azar (Ed.), Modeling and control of drug delivery systems (pp. 313–331). Academic Press. https://doi.org/10.1016/B978-0-12-821185-4.00007-5.

Bhattarai, M., Pitkänen, L., Kitunen, V., Korpinen, R., Ilvesniemi, H., Kilpeläinen, P. O., ... Mikkonen, K. S. (2019). Functionality of spruce galactoglucomannans in oil-inwater emulsions. Food Hydrocolloids, 86, 154–161. https://doi.org/10.1016/j. foodbyd 2018.03.020

- Bitter, T., & Muir, H. M. (1962). A modified uronic acid carbazole reaction. *Analytical Biochemistry*, 4(4), 330–334. https://doi.org/10.1016/0003-2697(62)90095-7
- Bradford, M. M. (1976). A rapid and sensitive method for the quantitation of microgram quantities of protein utilizing the principle of protein-dye binding. *Analytical Biochemistry*, 72(1), 248–254. https://doi.org/10.1016/0003-2697(76)90527-3
- Brodkorb, A., Egger, L., Alminger, M., Alvito, P., Assunção, R., Ballance, S., Bohn, T., Bourlieu-Lacanal, C., Boutrou, R., Carrière, F., Clemente, A., Corredig, M., Dupont, D., Dufour, C., Edwards, C., Golding, M., Karakaya, S., Kirkhus, B., Le Feunteun, S., ... Recio, I. (2019). INFOGEST static in vitro simulation of gastrointestinal food digestion. *Nature Protocols*, 14(4), 991–1014. https://doi.org/10.1038/s41596-018-0119-1
- Chen, L., Lin, X., Xu, X., Chen, Y., Li, K., Fan, X., Pang, J., & Teng, H. (2019). Self-nano-emulsifying formulation of Sonchus oleraceus Linn for improved stability: Implications for phenolics degradation under in vitro gastro-intestinal digestion: Food grade drug delivery system for crude extract but not single compound. *Journal of Functional Foods*, 53, 28–35. https://doi.org/10.1016/j.jff.2018.12.009
- Chen, Y., Yao, M., Peng, S., Fang, Y., Wan, L., Shang, W., Xiang, D., & Zhang, W. (2023). Development of protein-polyphenol particles to stabilize high internal phase Pickering emulsions by polyphenols' structure. *Food Chemistry*, 428, Article 136773. https://doi.org/10.1016/j.foodchem.2023.136773
- Cui, F., McClements, D. J., Liu, X., Liu, F., & Ngai, T. (2022). Development of pHresponsive emulsions stabilized by whey protein fibrils. Food Hydrocolloids, 122, Article 107067. https://doi.org/10.1016/j.foodhyd.2021.107067
- Danaei, M., Dehghankhold, M., Ataei, S., Hasanzadeh Davarani, F., Javanmard, R., Dokhani, A., ... Mozafari, M. R. (2018). Impact of particle size and polydispersity index on the clinical applications of Lipidic Nanocarrier systems. *Pharmaceutics*, 10 (2). https://doi.org/10.3390/pharmaceutics10020057
- Degrassi, A., Toffanin, R., Paoletti, S., & Hall, L. D. (1998). A better understanding of the properties of alginate solutions and gels by quantitative magnetic resonance imaging (MRI). Carbohydrate Research, 306(1), 19–26. https://doi.org/10.1016/S0008-6215 (97)10054-4
- Duan, X., Subbiah, V., Agar, O. T., Barrow, C. J., Ashokkumar, M., Dunshea, F. R., & Suleria, H. A. (2024). Optimizing extraction methods by a comprehensive experimental approach and characterizing polyphenol compositions of Ecklonia radiata. Food Chemistry., Article 139926. https://doi.org/10.1016/j.foodchem.2024.139926
- El-Sheekh, M. M., Deyab, M. A., Hassan, N. I., & Abu Ahmed, S. E. (2022). Green biosynthesis of silver nanoparticles using sodium alginate extracted from Sargassum latifolium and their antibacterial activity. *Rendiconti Lincei. Scienze Fisiche e Naturali*, 33(4), 867–878. https://doi.org/10.1007/s12210-022-01102-8
- Frent, O. D., Vicas, L. G., Duteanu, N., Morgovan, C. M., Jurca, T., Pallag, A., ... Marian, E. (2022). Sodium alginate-natural microencapsulation material of polymeric microparticles. *International Journal of Molecular Sciences*, 23(20). https://doi.org/10.3390/iims232012108
- Fuhrmann, P. L., Kalisvaart, L. C. M., Sala, G., Scholten, E., & Stieger, M. (2019). Clustering of oil droplets in o/w emulsions enhances perception of oil-related sensory attributes. Food Hydrocolloids, 97, Article 105215. https://doi.org/10.1016/ j.foodhyd.2019.105215
- Garcia-Campayo, V., Han, S., Vercauteren, R., & Franck, A. (2018). Digestion of food ingredients and food using an in vitro model integrating intestinal mucosal enzymes. Food and Nutrition Sciences, 9(6), 711–734. https://doi.org/10.4236/fns.2018.96055
- Geng, M., Li, L., Tan, X., Teng, F., & Li, Y. (2024). W/O/W emulsion-filled sodium alginate hydrogel beads for co-encapsulation of vitamins C and E: Insights into the fabrication, lipolysis, and digestion behavior. Food Chemistry, 457, Article 140095. https://doi.org/10.1016/j.foodchem.2024.140095
- Grande, R., & Carvalho, A. J. F. (2011). Compatible ternary blends of chitosan/poly(vinyl alcohol)/poly(lactic acid) produced by oil-in-water emulsion processing. Biomacromolecules, 12(4), 907–914. https://doi.org/10.1021/bm101227q
- Haddadzadegan, S., Dorkoosh, F., & Bernkop-Schnürch, A. (2022). Oral delivery of therapeutic peptides and proteins: Technology landscape of lipid-based nanocarriers. *Advanced Drug Delivery Reviews*, 182, Article 114097. https://doi.org/10.1016/j. addr.2021.114097
- Jia, N., Lin, S., Yu, Y., Zhang, G., Li, L., Zheng, D., & Liu, D. (2022). The effects of ethanol and Rutin on the structure and gel properties of whey protein isolate and related mechanisms. Foods, 11(21), 3480. https://doi.org/10.3390/foods11213480
- Jin, B., Zhou, X., Zheng, Z., Liang, Y., Chen, S., Zhang, S., & Li, Q. (2020). Investigating on the interaction behavior of soy protein hydrolysates/β-glucan/ferulic acid ternary complexes under high-technology in the food processing: High pressure homogenization versus microwave treatment. *International Journal of Biological Macromolecules*, 150, 823–830. https://doi.org/10.1016/j.ijbiomac.2020.02.138
- Khin, M. N., Goff, H. D., Nsor-Atindana, J., Ahammed, S., Liu, F., & Zhong, F. (2021). Effect of texture and structure of polysaccharide hydrogels containing maltose on release and hydrolysis of maltose during digestion: In vitro study. Food Hydrocolloids, 112, Article 106326. https://doi.org/10.1016/j.foodhyd.2020.106326
- Kim, W., Wang, Y., & Selomulya, C. (2022). Impact of sodium alginate on binary whey/pea protein-stabilised emulsions. *Journal of Food Engineering*, 321, Article 110978. https://doi.org/10.1016/j.jfoodeng.2022.110978
- Kim, W., Zia, M. B., Naik, R. R., Ho, K. K. H. Y., & Selomulya, C. (2025). Effects of polyphenols from Tasmannia lanceolata on structural, emulsifying, and antioxidant properties of pea protein. *Food Chemistry*, 464, Article 141589. https://doi.org/ 10.1016/j.foodchem.2024.141589

- Klinkesorn, U., & Julian McClements, D. (2010). Impact of lipase, bile salts, and polysaccharides on properties and digestibility of tuna oil multilayer emulsions stabilized by lecithin-chitosan. Food Biophysics, 5(2), 73–81. https://doi.org/ 10.1007/s11483-010-9147-2
- Kuang, Y., Xiao, Q., Yang, Y., Liu, M., Wang, X., Deng, P., ... Li, C. (2023). Investigation and characterization of Pickering emulsion stabilized by alkali-treated Zein (AZ)/ sodium alginate (SA) composite particles. *Materials*, 16(8), 3164. https://doi.org/ 10.3390/ma16083164
- Li, J., Geng, S., Zhen, S., Lv, X., & Liu, B. (2022). Fabrication and characterization of oil-in-water emulsions stabilized by whey protein isolate/phloridzin/sodium alginate ternary complex. Food Hydrocolloids, 129, Article 107625. https://doi.org/10.1016/ifoodhyd.2022.107625
- Li, S., Liu, Y., Qin, W., Zhang, Q., Chen, D., Lin, D., Liu, S., Huang, Z., & Chen, H. (2022). Physicochemical stability and in vitro bioaccessibility of β-carotene emulsions stabilized with arabinoxylan hydrolysates-soy protein isolate conjugates. *LWT*, 157, Article 113120. https://doi.org/10.1016/j.lwt.2022.113120
- Li, Y., Hu, M., Du, Y., Xiao, H., & McClements, D. J. (2011). Control of lipase digestibility of emulsified lipids by encapsulation within calcium alginate beads. Food Hydrocolloids, 25(1), 122–130. https://doi.org/10.1016/j.foodhyd.2010.06.003
- Liu, X., Qin, X., Wang, Y., & Zhong, J. (2022). Physicochemical properties and formation mechanism of whey protein isolate-sodium alginate complexes: Experimental and computational study. Food Hydrocolloids, 131, Article 107786. https://doi.org/ 10.1016/i.foodbyd.2022.107786
- Liu, Y., Liu, C., Zhang, S., Li, J., Zheng, H., Jin, H., & Xu, J. (2021). Comparison of different protein emulsifiers on physicochemical properties of β-carotene-loaded nanoemulsion: effect on formation, stability, and in vitro digestion. *Nanomaterials* (Basel), 11(1). https://doi.org/10.3390/nano11010167
- Luo, Z., Murray, B. S., Yusoff, A., Morgan, M. R., Povey, M. J., & Day, A. J. (2011). Particle-stabilizing effects of flavonoids at the oil-water interface. *Journal of Agricultural and Food Chemistry*, 59(6), 2636–2645. https://doi.org/10.1021/if1041855
- Najari, Z., Dokouhaki, M., Juliano, P., & Adhikari, B. (2024). Advances in the application of protein-polysaccharide-polyphenol ternary complexes for creating and stabilizing Pickering emulsions. *Future Foods*, 9, Article 100299. https://doi.org/10.1016/j. fufo.2024.100299
- Naumann, S., Haller, D., Eisner, P., & Schweiggert-Weisz, U. (2020). Mechanisms of interactions between bile acids and plant compounds—A review. *International Journal of Molecular Sciences*, 21(18), 6495. https://www.mdpi.com/1422-0067/21/18/6495
- Pal, R. (2024). Non-Newtonian behaviour of suspensions and emulsions: Review of different mechanisms. Advances in Colloid and Interface Science., Article 103299. https://doi.org/10.1016/i.cis.2024.103299
- Pang, Z., Sun, M., Li, B., Bourouis, I., Chen, C., Huang, Y., Liu, X., & Wang, P. (2024). Morphology, surface characteristics and tribological properties of whey protein/chitosan composite particles and their fat replacing effect in O/W emulsion. International Journal of Biological Macromolecules, 259, Article 129301. https://doi.org/10.1016/i.iibiomac.2024.129301
- Petrut, R. F., Danthine, S., & Blecker, C. (2016). Assessment of partial coalescence in whippable oil-in-water food emulsions. Advances in Colloid and Interface Science, 229, 25–33. https://doi.org/10.1016/j.cis.2015.12.004
- Pulat, M., & Ozukaya, D. (2019). Preparation and characterization of Na-alginate hydrogel beads. The Eurasia Proceedings of Science Technology Engineering and Mathematics.
- Rousi, Z., Ritzoulis, C., & Karayannakidis, P. D. (2014). Emulsion flocculation and stability in a simple in vitro gastrointestinal model. *Food Digestion*, 5(1), 1–7. https://doi.org/10.1007/s13228-013-0034-4
- Sarkar, A., Li, H., Cray, D., & Boxall, S. (2018). Composite whey protein–cellulose nanocrystals at oil-water interface: Towards delaying lipid digestion. Food Hydrocolloids, 77, 436–444. https://doi.org/10.1016/j.foodhyd.2017.10.020
- Sarkar, A., Ye, A., & Singh, H. (2016). On the role of bile salts in the digestion of emulsified lipids. Food Hydrocolloids, 60, 77–84. https://doi.org/10.1016/j. foodhyd.2016.03.018
- Setiowati, A. D., Vermeir, L., Martins, J., De Meulenaer, B., & Van der Meeren, P. (2016). Improved heat stability of protein solutions and O/W emulsions upon dry heat treatment of whey protein isolate in the presence of low-methoxyl pectin. Colloids and Surfaces A: Physicochemical and Engineering Aspects, 510, 93–103. https://doi. org/10.1016/j.colsurfa.2016.05.034
- Shen, S., Liu, X., Tang, D., Yang, H., & Cheng, J. (2024). Digestive characteristics of astaxanthin oil in water emulsion stabilized by a casein-caffeic acid-glucose ternary conjugate. *Food Chemistry*, 438, Article 138054. https://doi.org/10.1016/j. foodchem.2023.138054
- Soares, S. I., Goncalves, R. M., Fernandes, I., Mateus, N., & de Freitas, V. (2009). Mechanistic approach by which polysaccharides inhibit α-amylase/procyanidin aggregation. *Journal of Agricultural and Food Chemistry*, 57(10), 4352–4358. https://doi.org/10.1021/ij900302r
- Song, Y., & Yoo, S.-H. (2017). Quality improvement of a rice-substituted fried noodle by utilizing the protein-polyphenol interaction between a pea protein isolate and green tea (Camellia sinensis) extract. Food Chemistry, 235, 181–187. https://doi.org/ 10.1016/j.foodchem.2017.05.052
- Tang, S., Yang, X., Wang, C., & Wang, C. (2025). Effects of polyphenols on the structure, interfacial properties, and emulsion stability of pea protein: Different polyphenol structures and concentrations. *Molecules*, 30(8), 1674. https://doi.org/10.3390/molecules30081674

- Velderrain-Rodríguez, G., Fontes-Candia, C., López-Rubio, A., Martínez-Sanz, M., Martín-Belloso, O., & Salvia-Trujillo, L. (2023). Polysaccharide-based structured lipid carriers for the delivery of curcumin: An in vitro digestion study. Colloids and Surfaces B: Biointerfaces, 227, Article 113349. https://doi.org/10.1016/j.colsurfb.2023.113349
- Wang, W., Onnagawa, M., Yoshie, Y., & Suzuki, T. (2001). Binding of bile salts to soluble and insoluble dietary fibers of seaweeds. Fisheries Science, 67(6), 1169–1173. https://doi.org/10.1046/j.1444-2906.2001.00376.x
- Wang, X., Lin, Q., Ye, A., Han, J., & Singh, H. (2019). Flocculation of oil-in-water emulsions stabilised by milk protein ingredients under gastric conditions: Impact on in vitro intestinal lipid digestion. Food Hydrocolloids, 88, 272–282. https://doi.org/ 10.1016/j foodbyd 2018.10.001
- Wu, H., Liu, Z., Lu, P., Barrow, C., Dunshea, F. R., & Suleria, H. A. R. (2022). Bioaccessibility and bioactivities of phenolic compounds from roasted coffee beans during in vitro digestion and colonic fermentation. *Food Chemistry*, 386, Article 132794. https://doi.org/10.1016/j.foodchem.2022.132794
- Wu, L., Schroën, K., & Corstens, M. (2024). Structural stability and release properties of emulsion-alginate beads under gastrointestinal conditions. Food Hydrocolloids, 150, Article 109702. https://doi.org/10.1016/j.foodhyd.2023.109702
- Wu, M., He, X., Feng, D., Li, H., Han, D., Li, Q., ... Wang, J. (2023). The emulsifying properties, in vitro digestion characteristics and storage stability of high-pressure-homogenization-modified dual-protein-based emulsions. *Foods*, 12(22). https://doi.org/10.3390/foods12224141
- Xie, C., Leeming, M. G., Lee, Z. J., Yao, S., van de Meene, A., & Suleria, H. A. R. (2024). Physiochemical changes, metabolite discrepancies of brown seaweed-derived sulphated polysaccharides in the upper gastrointestinal tract and their effects on bioactive expression. *International Journal of Biological Macromolecules*, 272, Article 132845. https://doi.org/10.1016/j.ijbiomac.2024.132845
- Xie, H., Wei, X., Liu, X., Bai, W., & Zeng, X. (2023). Effect of polyphenolic structure and mass ratio on the emulsifying performance and stability of emulsions stabilized by polyphenol-corn amylose complexes. *Ultrasonics Sonochemistry*, 95, Article 106367. https://doi.org/10.1016/j.ultsonch.2023.106367
- Xu, J., Teng, F., Wang, B., Ruan, X., Ma, Y., Zhang, D., ... Jin, H. (2022). Gel property of soy protein emulsion gel: Impact of combined microwave pretreatment and covalent binding of polyphenols by alkaline method. *Molecules*, 27(11), 3458. https://doi. org/10.3390/molecules/27113458
- Xue, H., Feng, J., Tang, Y., Wang, X., Tang, J., Cai, X., & Zhong, H. (2024). Research progress on the interaction of the polyphenol–protein–polysaccharide ternary systems. Chemical and Biological Technologies in Agriculture, 11(1), 95. https://doi.org/10.1186/s40538-024-00632-7
- Yadollahi, Z., Motiei, M., Kazantseva, N., Císař, J., & Sáha, P. (2023). Whey protein isolate-chitosan polyelectrolyte nanoparticles as a drug delivery system. *Molecules*, 28(4), 1724. https://doi.org/10.3390/molecules28041724
- Yamaguchi, K., Itakura, M., Tsukamoto, M., Lim, S. Y., & Uchida, K. (2022). Natural polyphenols convert proteins into histone-binding ligands. *The Journal of Biological Chemistry*, 298(11), Article 102529. https://doi.org/10.1016/j.jbc.2022.102529
- Yan, J., Liang, X., Ma, C., McClements, D. J., Liu, X., & Liu, F. (2021). Design and characterization of double-cross-linked emulsion gels using mixed biopolymers: Zein and sodium alginate. Food Hydrocolloids, 113, Article 106473. https://doi.org/ 10.1016/j.foodbyd.2020.106473.
- Yan, X., Liang, S., Peng, T., Zhang, G., Zeng, Z., Yu, P., Gong, D., & Deng, S. (2020). Influence of phenolic compounds on physicochemical and functional properties of protein isolate from Cinnamomum camphora seed kernel. *Food Hydrocolloids*, 102, Article 105612. https://doi.org/10.1016/j.foodhyd.2019.105612
- Yang, M., Yang, Z., Everett, D. W., Gilbert, E. P., Singh, H., & Ye, A. Digestion of food proteins: the role of pepsin. Critical Reviews in Food Science and Nutrition, 1–22. doi:https://doi.org/10.1080/10408398.2025.2453096.
- Yang, W., Qu, X., Deng, C., Dai, L., Zhou, H., Xu, G., Li, B., Yulia, N., & Liu, C. (2021). Heat sensitive protein-heat stable protein interaction: Synergistic enhancement in the thermal co-aggregation and gelation of lactoferrin and α-lactalbumin. Food Research International, 142, Article 110179. https://doi.org/10.1016/j. foodres.2021.110179
- Ye, H., Chen, T., Huang, M., Ren, G., Lei, Q., Fang, W., & Xie, H. (2021). Exploration of the microstructure and rheological properties of sodium alginate-pectin-whey protein isolate stabilized B-carotene emulsions: To improve stability and achieve gastrointestinal sustained release. *Foods*, 10(9), 1991. https://doi.org/10.3390/ foods10091991
- Zhang, R., Zhang, Z., Zhang, H., Decker, E. A., & McClements, D. J. (2015). Influence of lipid type on gastrointestinal fate of oil-in-water emulsions: In vitro digestion study. Food Research International, 75, 71–78. https://doi.org/10.1016/j. foodres.2015.05.014
- Zhang, S., Murray, B. S., Holmes, M., Ettelaie, R., & Sarkar, A. (2023). Gastrointestinal fate and fatty acid release of Pickering emulsions stabilized by mixtures of plant protein microgels+cellulose particles: An in vitro static digestion study. Food Biophysics, 18(1), 120–132. https://doi.org/10.1007/s11483-022-09756-5
- Zhang, T., Huang, R., Xu, X., Chang, Y., & Xue, C. (2025). The characterization of fucoidan-sodium caseinate electrostatic complexes with application for pH-triggered release: Microstructure and digestive behavior. Food Research International, 207, Article 116076. https://doi.org/10.1016/j.foodres.2025.116076
- Zheng, Z., Luo, Y., Yao, L., Lu, J., & Bu, G. (2014). Effects of Maillard reaction conditions on the functional properties of WPI chitosan oligosaccharide conjugates. *Journal of Food Science and Technology*, 51(12), 3794–3802. https://doi.org/10.1007/s13197-013-0946-6